Ceiling fan air speeds around desks and office partitions

Yunfei Gao[a,b*], Hui Zhang[b], Edward Arens[b], Elaina Present[b], Baisong Ning[c], Yongchao Zhai[d], Jovan Pantelic[b], Maohui Luo[b,e], Lei Zhao[f], Paul Raftery[b], Shichao Liu[b]

[a] *School of Architecture and Urban Planning, Guangdong University of Technology, Guangzhou, Guangdong, 510090, PR China*

[b] *Center for the Built Environment, University of California at Berkeley, Berkeley, CA 94720, USA*

[c] *College of Civil Engineering, Hunan University, Changsha, Hunan, 410082, PR China*

[d] *College of Architecture, Xi'an University of Architecture and Technology, Xi'an, Shaanxi, 710055, PR China*

[e] *Department of Building Science, Tsinghua University, Beijing 100084, PR China*

[f] *School of Municipal and Environmental Engineering, Xi'an University of Architecture and Technology, Xi'an, Shaanxi, 710055, PR China*

Abstract

Ceiling fans may cool room occupants very efficiently, but the air speeds experienced in the occupied zone are inherently non-uniform. Designers should be aware of several generic flow patterns when positioning ceiling fans in a room. Key to these are the fan jet itself and lateral spreading near the floor. Adding workstation furniture redirects the jet's airflow laterally in a deeper spreading zone, making room air flows more complex but potentially increasing the cooling experienced by the occupants.

This paper presents the first evaluation of the effects of tables and workstation partitions on a room's generic air flow and comfort profiles. In a test room with a ceiling fan, we moved five anemometers mounted in a "tree" at heights of 0.1, 0.6, 0.75, 1.1, and 1.7 m to sample a dense measurement grid of 7 rows and 6 columns. We tested five different table and partition configurations and compared them to the empty room base case. From the results we propose a simplified model of room airflow under ceiling fans, useful for positioning fans and workstation furniture. We also present comfort contours measured in two ways that have comfort standards implications. The measured data are publicly available on the internet.

Keywords: Ceiling fan; air speed; furniture; comfort cooling; corrective power

Highlights

1. We performed high resolution measurements of ceiling-fan-induced air flow in an empty room;
2. We compare this reference case to air flow profiles measured in the room with five different table and partition configurations. The data are included as publicly available supplementary material;
4. The initial ceiling fan flow in the room could be modeled as a free jet;
5. The subsequent room circulation, with and without tables and partitions, may be represented by an intuitive model for designers who are placing fans and furniture;
6. The extent of comfort cooling provided by the fan air flow can be represented by the metric 'corrective power'. Corrective power equates the cooling effect of the fan as an ambient temperature reduction, °C. We present the corrective power distribution in the room in two ways--with and without the air speed at ankle level--to evaluate air speed cooling effect. This evaluation is significant for thermal comfort standards.

1. Introduction

Designers can use air movement to extend the thermal comfort range in the built environment, as per ASHRAE Standard 55, *Thermal Environmental Conditions for Human Occupancy* [1][2]. In buildings with mechanical cooling systems, increased air movement allows the mechanical cooling systems to operate fewer hours over the course of the year, and at lower power during operation, yielding significant energy savings[3][4][5][6][7]. In buildings without mechanical cooling systems, the number of comfortable hours increases when air movement is incorporated into the design. Air movement is not a second-rate or undesirable cooling mechanism; Zhang et al. [8], Arens et al. [9], and Toftum [10] showed that a majority of occupants surveyed in offices preferred having more air movement than less in both neutral and warm environments.

The size of the cooling effect produced by air movement depends upon the speed of the air at the surface of the occupants' skin [11], [12]. To use air movement effectively throughout a space, designers must have knowledge of the air speed patterns in the occupied zone produced by air movement sources. The ceiling fan is a source that in recent years has become highly effective and energy-efficient.

A few previous studies of ceiling fans have addressed the room air speed profiles they cause. Sonne and Parker [13] experimentally measured air speed profiles in a closed room for four commercially available ceiling fan types. Jain et al. [14] experimentally developed quantitative profiles, qualitative descriptions, and visualizations for flow in a closed room with a ceiling fan. Bassiouny and Korah [15] developed an analytical and computational model to predict the airflow from a ceiling fan operating at different speeds. All of these studies were characterizing the flow from a single ceiling fan operating in an empty room.

In actual buildings, rooms usually contain obstacles to airflow such as furniture and occupants. These have the potential to significantly affect the air speed profiles produced by the ceiling fans, and therefore also the cooling and comfort that occupants experience at different locations in the room. Two studies have considered the effect of obstacles on ceiling fan air speed profiles. Ho et al.[16] did numerical CFD simulations to evaluate 2D and 3D airflow and heat transfer profiles in a room. The room contained an air conditioner, a ceiling fan, and a person standing under the fan. The experimental variable was the speed of the fan, not the location of the person. Scheatzle et al. [17], as part of determining where to place subjects for their thermal comfort experiment, took air speed profile measurements in a room with desks. However, the paper does not quantitatively report these measurements. While these two studies did model or measure air speed profiles in rooms with obstacles, we are not aware of any studies that evaluate the effects of obstacle location on the air speed profiles in the room. Obstacle effects on comfort cooling have also not been reported in the literature.

At this time, a standard is under development by ASHRAE TC 216 for testing ceiling fans, and for providing guidance for positioning such fans within rooms to optimize comfort. There is almost no literature available for developing this design guidance. There are also amendments in progress within Standard 55 addressing how airflows that are not uniformly distributed across the body might affect comfort. Although some literature [7], [22], [26] has quantified the cooling under airstreams that only partially cover the body, there is no current guidance for translating such results into the metrics used in standards.

One might identify three problems that need to be solved:

1. Absence of any measured fan-driven airflow data for spaces containing furniture.
2. Need for a simplified organizing model of room airflow to help designers position ceiling fans and workstations beneath them.
3. Need for a general approach to assessing human cooling and comfort in non-uniform airstreams, and in particular the comfort occurring around desktops and workstation partitions.

The objective of this study is to reveal air flow patterns that might be used in positioning fans and workstation furniture to achieve effective cooling of occupants. The approach is to experimentally measure and visualize air speed profiles around furniture placed in different locations in the ceiling fan airflow path, and to compare them to profiles for the empty room. The focus is on the lower occupied levels of the room. Using these measurements, it should be possible to develop a simplified model of air flow in a furnished room, and to define further measurements that might extend the model to include multiple fans and additional furniture arrangements. It should also be possible to characterize the effect of measurement heights that are used in the comfort standard. Finally, the data are to be made publicly available for simulation validation.

2. Methods

2.1 Testing facilities

A test chamber (L x W x H: 5.49 x 5.49 x 2.53 m, 18 x 18 x 8.3 ft) provided a realistic office-like space for measuring airflow from ceiling fans (Figure 1). We tested a 1524 mm diameter ceiling fan (Haiku, Big Ass Solutions), installing it at the center of the chamber along the north-south direction, but off-center along the west-east direction due to a duct in the overhead plenum blocking a central attachment point. The fan was 2.15 m from the east wall and 3.35 m from the west wall. The distance of the ceiling fan blade to the top of the ceiling was 0.235 m, 15.4% of the fan diameter; greater than the 'starvation distance' needed to assure efficient fan operation. The fan has 6 speed levels ranging in input power from 2 W to 16 W, and 70.5 to 175 RPM. We performed the empty room test at levels 2, 4, and 6, and all furnished tests were performed at speed level 4 (6 W, 121 RPM).

We measured air speed using five omnidirectional anemometers mounted in a vertical tree (Figure 1). The anemometer system, manufactured by Sensor Inc., is designed for the typically low air speeds in room flow with an accuracy ±0.02m/s or 1% of reading (0.05 – 5 m/s). Moving the tree allows the capture of the airflow distribution over the floor area. We acquired the data with a sampling frequency of 0.5Hz. Temperatures at all measurement points within the chamber were isothermal, within 0.5C.

Figure 1: Experiment setup

2.2 Test cases

We evaluated the air speed profiles or various configurations of a single ceiling fan with and without furniture. These were: no table, a single table at seated- and standing-height, and various table positions relative to the ceiling fan, as well as two types of partitions around the table. This paper only presents the results for the seated-height table. Figure 2 summarizes the test configurations of 6 cases. The light grey grid crossing points in the figures represents the air speed measurement locations, 30 cm apart, described in more detail later in the paper. The capital letters indicate the chamber orientation, N - north, S - south, E - east and W – west.

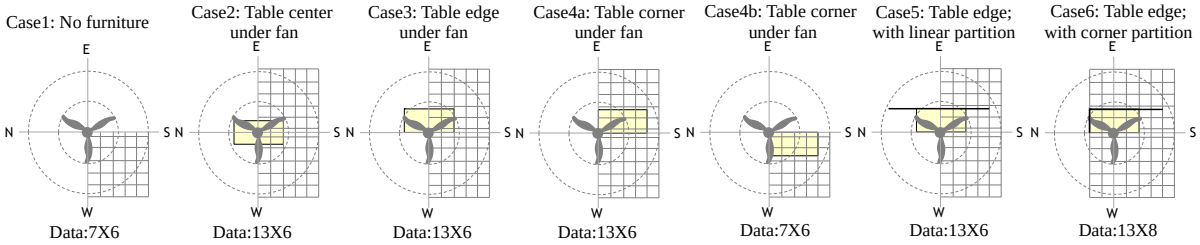

Figure 2: *The test cases viewed from above, with fan rotating clockwise*

Case 1 is the base case condition as it does not include any furniture. Cases 2 – 4 represent configurations for various table locations relative to the ceiling fan. Case 2 has the table directly underneath the ceiling fan with the center of the fan above the center of the table. Case 3 positions the fan to one side of the table – the center of the fan is above the center of the long edge of the table. Case 4 positions the fan over a corner of the table. This is the only case in which the table is not entirely under the disk of the fan. Since the fan airflow swirls in the direction of fan rotation, there might be different airflows over the table depending on whether the swirl encounters the longer or shorter side of the table. We therefore tested two configurations, with the swirling air approaching the shorter side of the table (Case 4a), and with the air approaching the longer side (Case 4b). The next two cases involved configurations with a partition bordering the table (represented by the black lines in Fig 2); Case 5 with a linear partition and Case 6 with a corner partition.

A typical sitting table height is 0.75 m [13] [14]. The table surface area is 0.6 m x 1.2 m. The partitions' height is 1.4 m, extending 0.65 m above the table top. The linear partition is 2.4 m long, and the L-shaped corner partition dimensions are 0.6 m x 1.8 m.

2.3 Flow visualization

In order to visualize the ceiling fan flow pattern and plan the air speed measurement points, we released theater fog directly upstream of the fan disk to characterize the boundaries and direction of the jet, as shown in Figure 3. The chamber surfaces were covered with matte black paper to provide contrast. Room temperature was isothermal, and the fan speed was level 4, the same as most of the subsequent testing.

We also released fog through a long linear smoke comb that traversed the jet into the surrounding still air, to detect the local streamlines around the jet. In the Case 4 tests, we also characterized the planar flow at tabletop using a moveable incense stick on the table (described later).

Chamber without table Chamber with table

Figure 3. Visualization of the fan jet's flow boundaries with and without a table

2.4 Air speed measurement

Anemometers were mounted on the tree at five heights: 0.1 m, 0.6 m, 0.75 m, 1.1 m and 1.7 m from the floor. Four of the heights (0.1, 0.6, 1.1, 1.7 m) are specified in comfort standards for representing seated and standing people, and the 0.75 m measurement captures the flow over the top of the table.

The measurement area extends 2 times the radius of the fan blades from the center of the fan towards the south, west, or east wall. For the six test cases, the sensor tree took measurements at the intersection of the light-grey grid lines shown in Figure 2. Each of the test quadrants (e.g. from center to south and west), the measurement grid is 7 rows x 6 columns, with 30 cm spacing. In Cases 2 – 6, the measurements begin 10 cm away from the edge of the table so that we capture the air speed experienced by people sitting near the table. We also always measured the row along the center of the fan. Therefore, the row positions are 0.0m, 0.1m[1], 0.4 m[2], 0.7 m[3], 1.0m, 1.3 m and 1.6 m from the fan center. The column

[1] West edge of the table plus 10 cm for Cases 3 & 4.
[2] East and West edges of the table plus 10 cm for Case 2; West edge of the table plus 10 cm in Cases 5 & 6.
[3] East edge of the table plus 10 cm for Cases 3 & 4.

positions are 0.0m, 0.3m, 0.6 m, 0.9m, 1.2m and 1.5 m from the fan center. Position 0 represents the center of the fan. We denote the row positions as R-0, R-0.1, R-0.4, R-0.7, R-1.0, R-1.3, R-1.6, and the column positions as C-0, C-0.3, C-0.6, C-0.9, C-1.2 and C-1.5.

We used Tecplot software to graph the measured air speed contours in horizontal and vertical cross sections. The data between measurement points were filled in by inverse distance weighting using the data from nearby measurement points. In some cases we took additional measurements near highly variable flow locations, like the corner of the table, to make the plot lines more accurate. For the contour images, distance from the fan center towards the east or south is represented as positive, and towards the west or north is negative.

3. Results

Each test case is associated with airspeed graphs and a set of horizontal and vertical contour maps. In the *results* section here, we present Cases 1, 3, and 6 in detail: the empty room base case, a table, and a table plus partition. These are described by an air speed profile plot, and by some examples of the vertical and horizontal contour plots collected for each case. The other cases (2, 4, and 5) are described in shortened form, focusing on observed differences from the detailed cases. The complete set of vertical and horizontal contours for all the cases is presented in *Appendix A*. The data are included as supplementary material, public available.

3.1 Case 1: Base case, no furniture

This base case was measured at higher resolution than the rest of the testing because the fan jet drives the rest of the flow in the chamber. Figure 4 shows the air speed profile at the cross section along the fan center line (R-0), generated from a set of measurements taken at 10 heights, 10 cm apart along the fan-center line to 5 cm from the south wall.

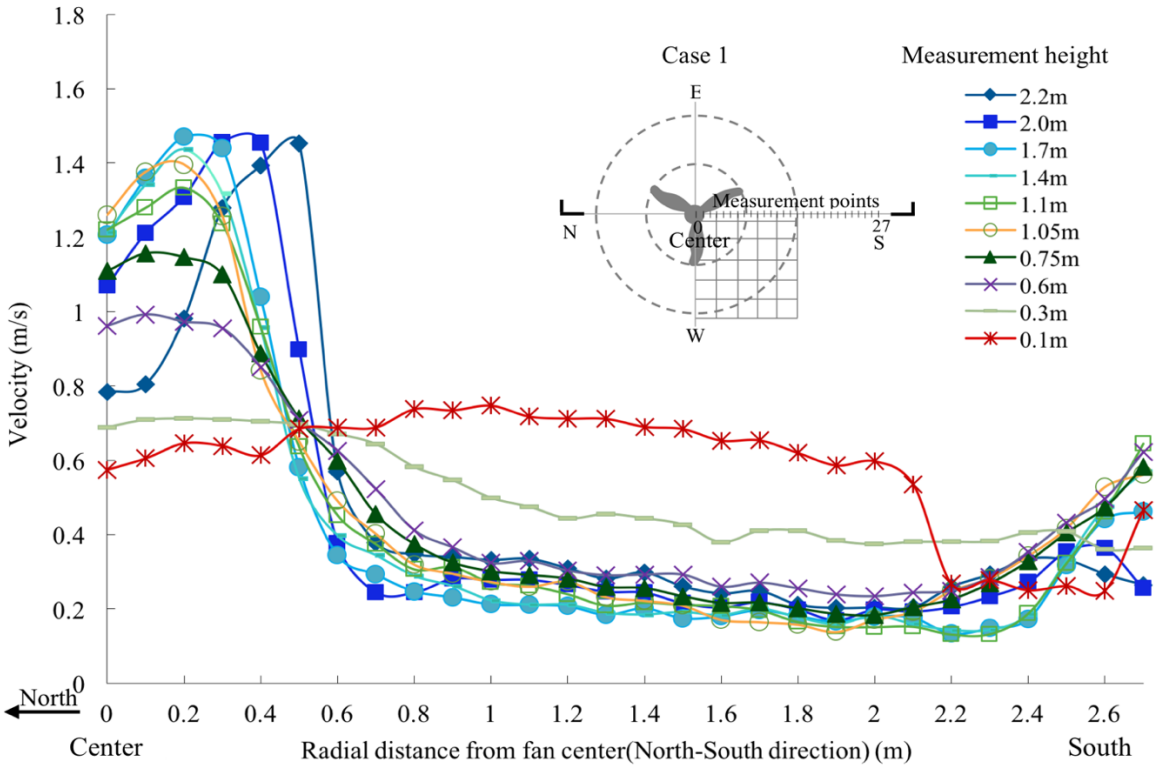

Figure 4: Fan profiles along the center-line, Case 1

The following are key observations about Figure 4. First, the *outer boundary* of the air flow jet descending from the ceiling fan does not spread beyond the diameter of the blade tips until it passes below 0.6 m from the floor (see the purple line in Figure 4). Between the fan and 0.6 m height, the jet is a very gradually widening cone that remains within the fan blade diameter. It might also be viewed as a simple cylindrical column (see Figure 3). The speed within the column is high, and outside it is low, between 0.15 – 0.3 m/s.

The propeller blades create a ring jet with a *hollow center*. The peak air speed just below the fan occurs 0.5 m from the fan center (70% of the 0.75 m fan blade radius). The hollow in the center fills in as the jet moves towards the floor, and this acts to confine the outer diameter of the jet described above. At the 1.1 m height, the peak speed happens at 0.2 m from the fan center (30% of the fan blade radius), and the peak-to-hollow difference is much diminished. At the 0.6 m height, the peak and hollow are barely distinguishable.

When the jet encounters the horizontal floor surface, its speed is slowed as it changes direction due to *impingement*. At 0.3 m above the floor the speed is evenly distributed across the jet at 0.7 m/s, about half the jet's starting speed. At 0.1 m height above the floor, the air speed within the jet can be seen to be slightly lower (about 0.6 m/s) than the speed outside of the fan blade diameter (about 0.7 m/s). Momentum redistribution causes lower speed in the impingement region, compared to the directionally well-defined outwash spreading radially outward from the cylindrical fan jet near the floor. This will also be seen later in cross sections for other fan speed levels. The speed of the spreading flow is greatest at the lowest levels (e.g., the 0.1 m red line in Figure 4).

A second impingement occurs as this horizontally spreading flow reaches the walls of the chamber and is redirected upward along the wall. The 0.1-m-level air speed drops sharply from 0.6 to 0.25 m/s around 0.5 m from the wall. The drop is not as pronounced at the 0.3 m height, where the speed of the spreading flow is much lower.

In the S. Beltaos and N. Rajaratnam [18][19][20] empirical model for circular turbulent impinging jets, the height of an impingement zone is 0.14H (H is the height, or distance, between the jet nozzle and the impinging surface), and the impinging region covers an area with radius 0.22H. The height of the ceiling fan in our test is 2.3 m. Using the above equations, the height of the impingement zone is 0.3 m, and the impingement region radius is 0.22H = 0.5 m. These predictions are quite similar to our measurements.

From the literature [11] and our own measurement results, we might view the flow field for a ceiling fan in a room as having five zones: the fan jet itself, the floor impingement zone, the outward spreading zone along the floor that is 0.3-0.5 m deep, the upward flowing wall zone, and a large still-air zone with a net motion that is very slowly upward (Figure 5). Placing furniture on the floor will create new flow impingement surfaces and alter these zone boundaries.

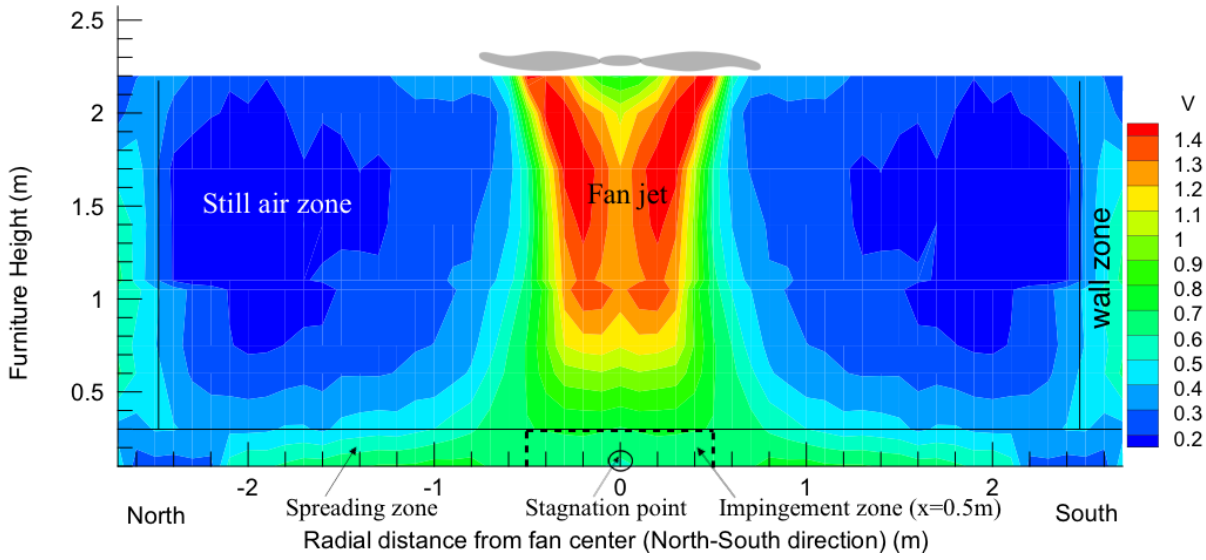

Figure 5: Vertical air speed contour through center of fan, Case 1

Horizontal contours at all heights: Figure 6 shows the horizontal air speed contours at 1.7 m, 1.1 m, 0.75 m (table height), 0.6 m, and 0.1 m. Using 0.3 m/s as the threshold airspeed defining the boundary between the jet and still air, the jet covers an area about the size of the fan diameter for all but the lowest height. We use 0.3 m/s because it is the lowest air speed capable of penetrating the rising thermal plume that surrounds the human body, and it can be distinctly perceived by occupants as providing cooling in neutral to warm environments.

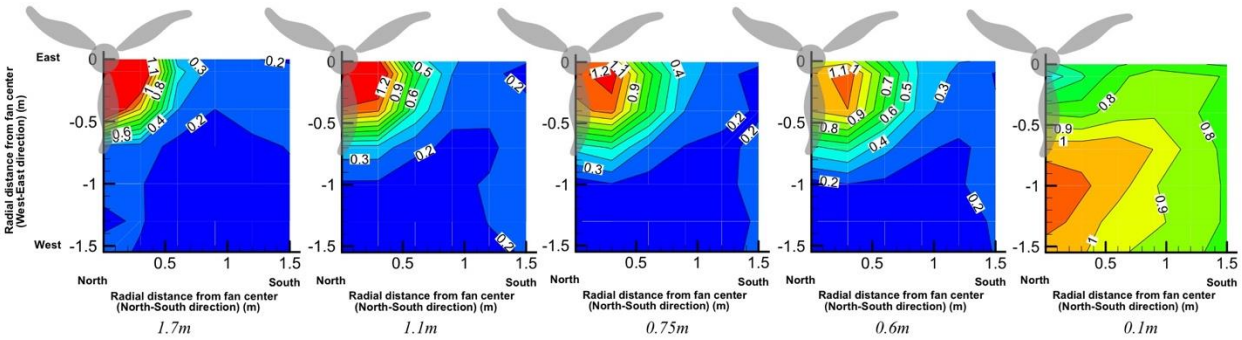

Figure 6: Horizontal air speed contours at 1.7 m, 1.1 m, 0.75 m (table height), 0.6 m, and 0.1 m, Case 1, without table (X, Y axes are distance from the fan center, m)

Table 1 summarizes the fan jet coverage area for all but the lowest height. As the jet flows down from 1.7 m to 0.6 m, its radius increases from 0.7 m to 1.0 m (west) or 1.1 m (south), and the air speed maximum reduces from 1.5 m/s to 1.1 m/s. The slight non-circularity of the jet and its outflow at floor level appears to be caused by the non-central position of the fan within the room.

Table 1: Flow spread area for different heights using 0.3 m/s as the threshold, Case 1

Schematic	1.7 m	1.1 m	0.75 m	0.6 m
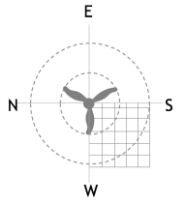	R_{west}=0.7 m C_{south}=0.7 m V_{max}=1.5 m/s	R_{west}=0.8 m C_{south}=0.9m V_{max}=1.3 m/s	R_{west}=0.9m C_{south}=1.0m V_{max}=1.2m/s	R_{west}=1.0m C_{south}=1.2m V_{max}=1.1 m/s

Air speed averages at three and two heights associated with occupant cooling. Corrective power equates the cooling effect of the fan as an ambient temperature reduction, ºC [7]. Figure 7a-d show averages of the air speeds affecting a seated occupant. Figure a and b average the speeds for the three (0.1, 0.6, and 1.1m) heights specified for seated occupants in ASHRAE Standard 55 and compute the corrective power comfort metric [7][1][21]. Figures c and d average the two heights (0.6 and 1.1 m) at which the body has the greatest surface area for cooling. [4]

Figure 7a shows that the average velocity for 0.1m, 0.6m and 1.1m exceeds 0.3 m/s over a circular region having twice the fan blade diameter. This spreading of fan cooling effect beyond the jet boundary is caused almost entirely by the contribution of horizontally spreading air velocity at 0.1 m height (see Figure 6). The corresponding corrective power contour is plotted in Figure 7b. By excluding the ankle-level air speed in Figures 7c and d, the fan's cooling effect is limited to be almost entirely within the fan blade diameter.

[4] Corrective power has been evaluated for vertical and horizontal air flows that uniformly affect the body, and for flows in impacting only the upper body, which for a given air speed produce CP's similar to uniform flows [22]. CP's for flow profiles in which the ankle-level airspeed is highest have not been studied to date. This will be addressed in the Discussion section below.

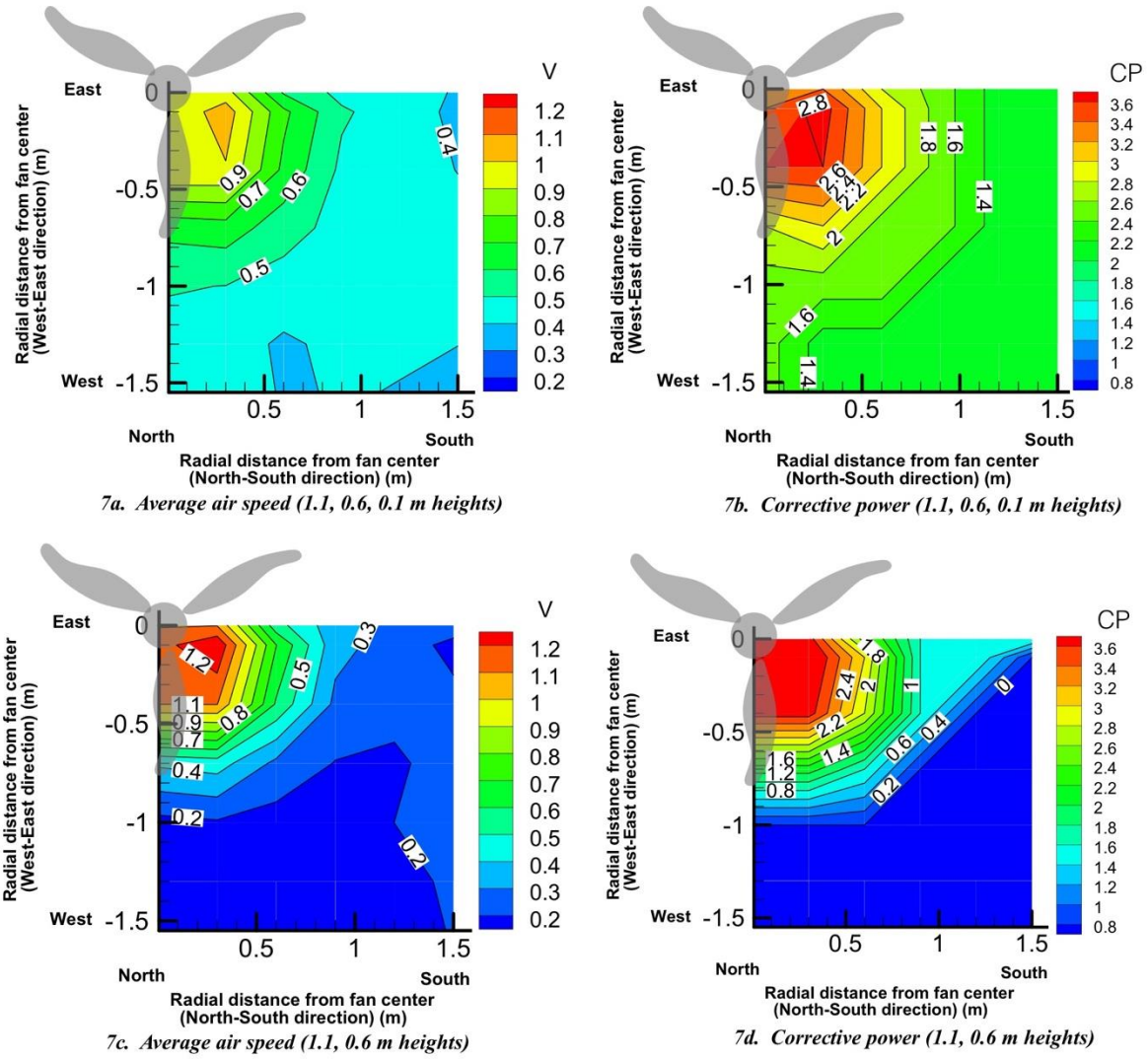

Figure 7a, b: average speed and corrective power contours for 1.1, 0.6, 0.1 m average height; 7c, d: average speed and corrective power contours for 1.1, 0.6 m average height

Effect of fan speed. All the results presented above are for the fan running at level 4 (121 RPM). We also evaluated the Case 1 air speed profiles for fans running at level 2 (70.5 RPM) and level 6 (175 RPM), without any furniture as above. The results are presented in Figure 8.

Compared to fan level 4 (Figure 4), the profiles are strikingly similar, except that the air speed magnitudes vary. The peak-to-hollow differences appear all the way down to 0.6 m from the floor. For the fan levels 4 and 6 (Figure 4 and Figure 8), the peaks appear between 0.2 – 0.3m from the center. When the air speed is lower (fan level 2), the air flow spreads slightly more, with the peaks between 0.3 – 0.5m. At 0.1m height, a uniform higher air speed covers most of the floor area across the room, 0.6 m from the wall, for all three fan levels. At level 2, however, these spreading air speeds would become imperceptible, not much higher than still air.

The constancy of fan flow profiles at different speeds is encouraging, in that it suggests that a ceiling fan flow model might be generalized to be independent of fan speed.

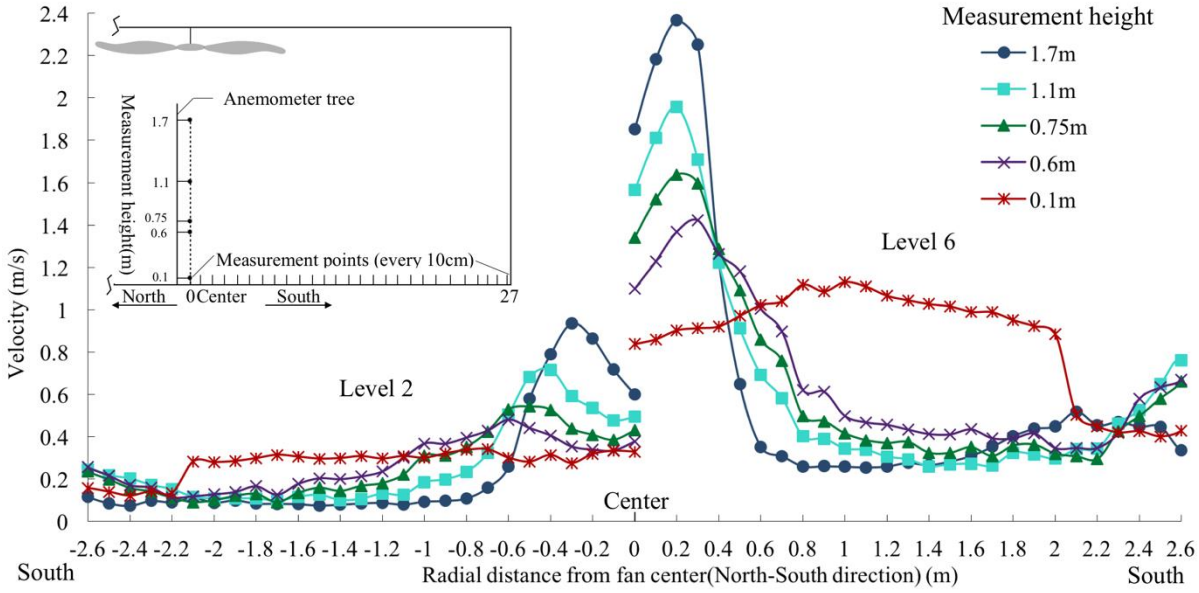

Figure 8. Air speed profiles at fan levels 2 and 6 for Case 1

3.2 Case 2: Fan centered above table midpoint

In Case 2, a 0.6 x 1.2 m table is centered directly under the fan jet. The tabletop surface moves some of the jet's impingement zone upward, to just above the 0.75m height of the table. Much of the jet is forced to spill outward over the tabletop as seen in Figure 3b. Figure 9 shows the table in two sections.

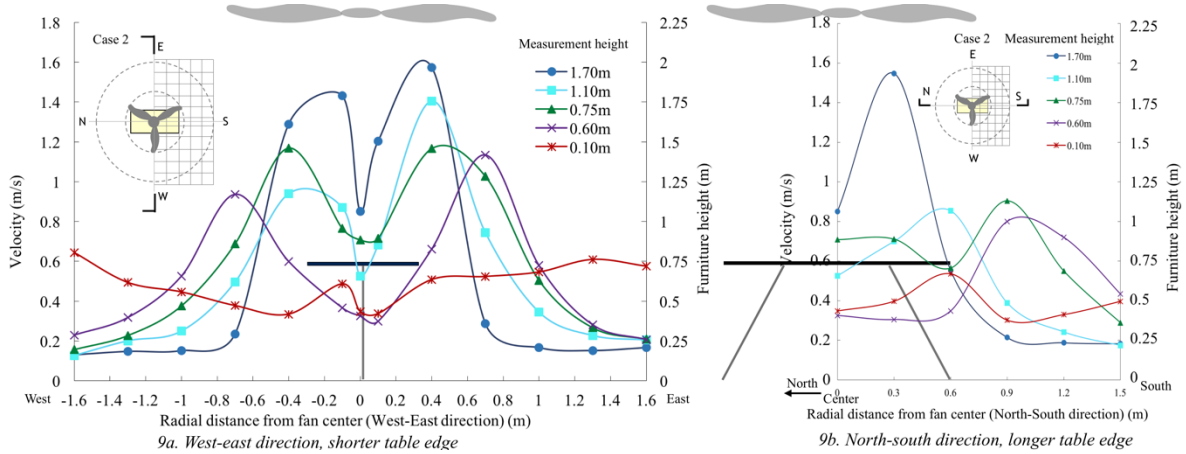

Figure 9: Case 2 velocity profiles along the fan centerline, west-east (a, left) and north-south (b, right).

Figure 9a gives air speed profiles across the shorter table length (0.6 m, west-east direction) on the fan center line. For the speed profiles at table height and above (0.75, 1.1, and 1.7 m height), the maximum peak speed locations shift from 0.2 m in Case 1 (Figure 4) to 0.3 to 0.4 m in Case 2, right outside of the table edge. For the 0.6 m mid-body height just below

tabletop level, the peak locations move out even further, to 0.4 m from the edge of the table, or 0.7 m from the fan center.

For the air speed profile across the longer table length (1.2 m, north-south direction) on the fan center line, the peak speed at the 1.7 m height is at 0.3 m from fan center, and by the 1.1 height has moved laterally to the edge of the table, 0.6 m from the fan center. Unlike the profile along the short table center line (Figure 7a), where only the air speed at the 0.6m height extends into the occupied zone away from the table edge, the profile along the longer side of the table produces peak air speeds at both 0.75 m (table height) and 0.6 m beyond the edge of the table. This is because the air spilling over the more distant table edges has turned more toward the horizontal than the flow over the closer edges that are still under the downward jet of the fan.

All air speeds (not only the peak values) move outwards from the fan center. For the 1.1 m height, at 0.6 m distance from the fan center, the speed increases from 0.45 m/s in Case 1 to almost 1 m/s in Case 2. Again using 0.3 m/s as the threshold speed, the coverage diameter can be seen to increase from 0.8 m in Case 1 to 1.1 m in Case 2. In Case 1 at the tabletop height (0.75 m) the speed is 0.9 m/s to 0.3 m/s for locations within 0.4 – 1m from the fan center. With the table present at these locations, the speed is 1.2 m/s to 0.5 m/s, a significant increase. At 0.7 m from the fan center in Case 1, the speed is around 0.4 m/s; in Case 2, it is still as high as 1 m/s. In Case 1 at 0.6 m height, the speed drops rapidly from 1 m/s at 0.4 m to 0.3 m/s at 1 m from fan center, while in Case 2 the speeds are all above 0.6 m/s in this region. At the 0.1 m height the speeds in Case 2 are similar to those in Case 1.

3.3 Case 3: Fan centered above table long edge

Figure 10 shows the fan central profiles along the east-west and north-south directions. The east-west profile cuts through the table, and the north-south profile shows the air speed along the long edge of the table.

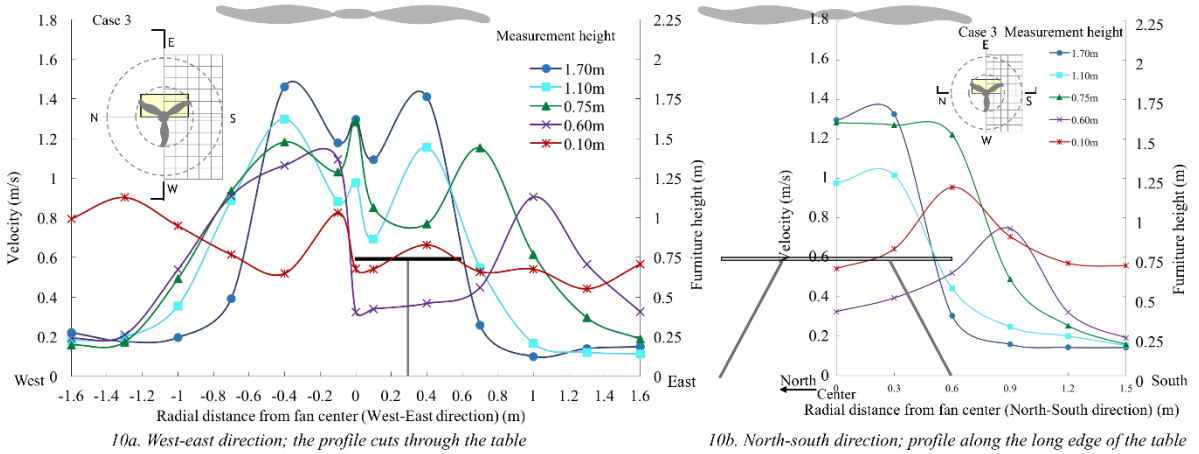

10a. West-east direction; the profile cuts through the table

10b. North-south direction; profile along the long edge of the table

Figure 10: Case 3 air speed profiles along the fan centerline; west-east (a, left) and north-south along the longer west edge of the table (b, right).

Figure 10a shows that the peak air speeds on the table side (east, right side of the figure) are lower than the speeds on the side without the table (west, left side of the figure), but that the

jet spreads much further and follows a spilling trajectory over the table edge. At 1.7 m and 1.1 m height, the maximum air speeds are located around 0.4 m from the fan center as they are in Case 2 (Figure 9a) when the table is centered under the fan. As with Case 2, the maximum air speed for the 0.75 m height is at the edge of the table, and the maximum for the 0.6 m height is 0.4 m from the table edge.

On the west side (where the jet is not blocked by the tabletop), the air speed peaks for the different heights are almost all located at the same distance from the fan center, about 0.4 m. This is further from center than in Case 1 (0.2m) showing the influence of the table in deflecting the flow to the west. There is an additional set of peaks under the fan center due its being directly above the edge of the table. At 0.7 m from the fan center, the air speeds for 1.1, 0.75, and 0.6 m increase from near 0.4 m/s in Case 1 to above 0.9 m/s in Case 3. The air speed at 0.1 m height is significantly greater than in Case 1 and Case 2, especially on the free flow side (without table, west side).

Figure 10b shows the north-south direction air flow profile along the fan center, which is along the table's long edge. The measurements were done on the south side. The table is presented as an open line, since the profile does not cut through the table.

The most interesting air speeds occur at table height (0.75 m) along the edge of the table. They are high, about 1.3 m/s, and are uniform without peaks. This indicates that the table dominates the air flow near the table edge: when the ceiling fan jet impinges on the table, the air is deflected along the table surface and jets over the edges quite equally. This agrees with the 0.75 m peaks in Case 2 (Figure 9a) and Case 3 (Figure 10a); all of these show the maximum speed directly at the edge of the table.

Vertical contours: The west-east vertical air speed contour centered under the fan (Figure 11) corroborates the Figure 10a profiles, showing the outward spread of the jet over the table surface. On the west side the jet is deflected slightly less, though the total flow to this side is increased by the presence of the table. The impingement zone above the table top is visible as a reduced velocity.

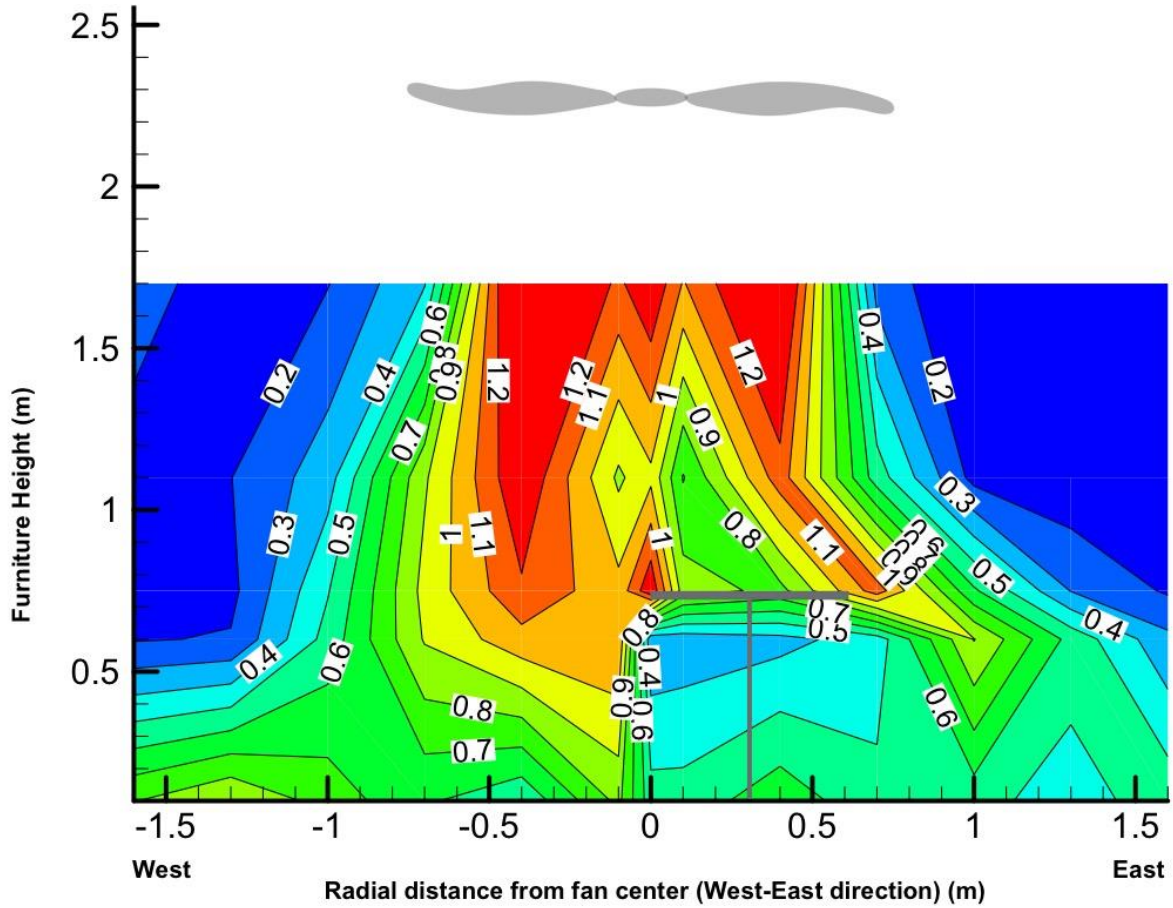

Figure 11. Vertical air speed contour through center of fan (C-0). The table is represented by the "T" shape.

Horizontal contours at all heights: Figure 12 shows horizontal air speed contours at 1.1 m, 0.75 m (table height), and 0.6 m. For the 0.75 m and 0.6 m heights, the speeds on the table side (east side) are smaller than those on the non-table side (west side), but are more uniform and cover greater areas. Comparing with Figure 6 (horizontal contour at 0.75 m height for Case 1), the air speed on the table side (east side) extends about 20 – 40 cm further outward, which is the same distance as the offset of the edge of the table toward the east. The contours on the side without the table do not extend as much, except along the south-side table edge, forming a triangular elevated air speed region rather than the round-shaped region shown on the non-table side.

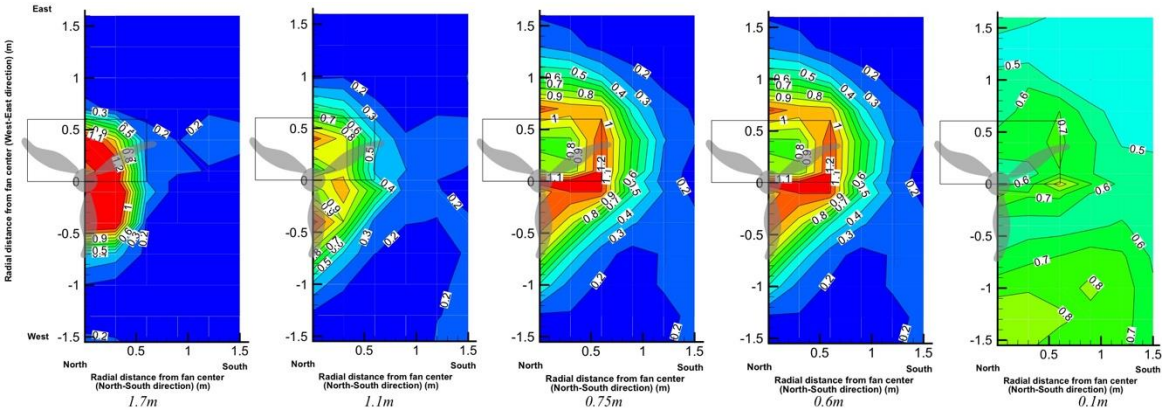

Figure 12: Horizontal air speed contours at 1.7 m, 1.1 m, 0.75 m (table height), 0.6 m, and 0.1 m, Case 3, fan centered above table long edge (X, Y axes are distance from the fan center, m)

Table 2 summarizes the air speed coverage regions for the 0.3 m/s threshold at different heights. The regions are characterized by the radius of round shaped or the length of triangular regions. There is no triangular-shaped profile at the 1.7 m height, indicating that the table is not impacting the profile at that height.

Table 2: Flow spread area for different heights using 0.3 m/s as the threshold, Case 3

Table beside fan	1.7 m	1.1 m	0.75 m	0.6 m
Table side	R_{east}=0.7 m C_{south}=0.6 m Quarter circle area V_{max}=1.4 m/s	R_{east}=0.9 m C_{south}=0.9 m Quarter circle area V_{max}=1.2 m/s	R_{east}=1.3 m C_{south}=1.2 m Quarter circle area V_{max}=1.3 m/s	R_{east}>1.5 m C_{south}=1.3 m Quarter circle area V_{max}=1.0 m/s
No table side	R_{west}=0.7 m C_{south}=0.6 m Quarter circle V_{max}=1.6 m/s	R_{west}=1.1 m C_{south}=0.9 m Triangle V_{max}=1.3 m/s	R_{west}=1.2 m C_{south}=1.2 m Triangle V_{max}=1.2 m/s	R_{west}=1.2 m C_{south}=1.3 m Triangle V_{max}=1.1 m/s

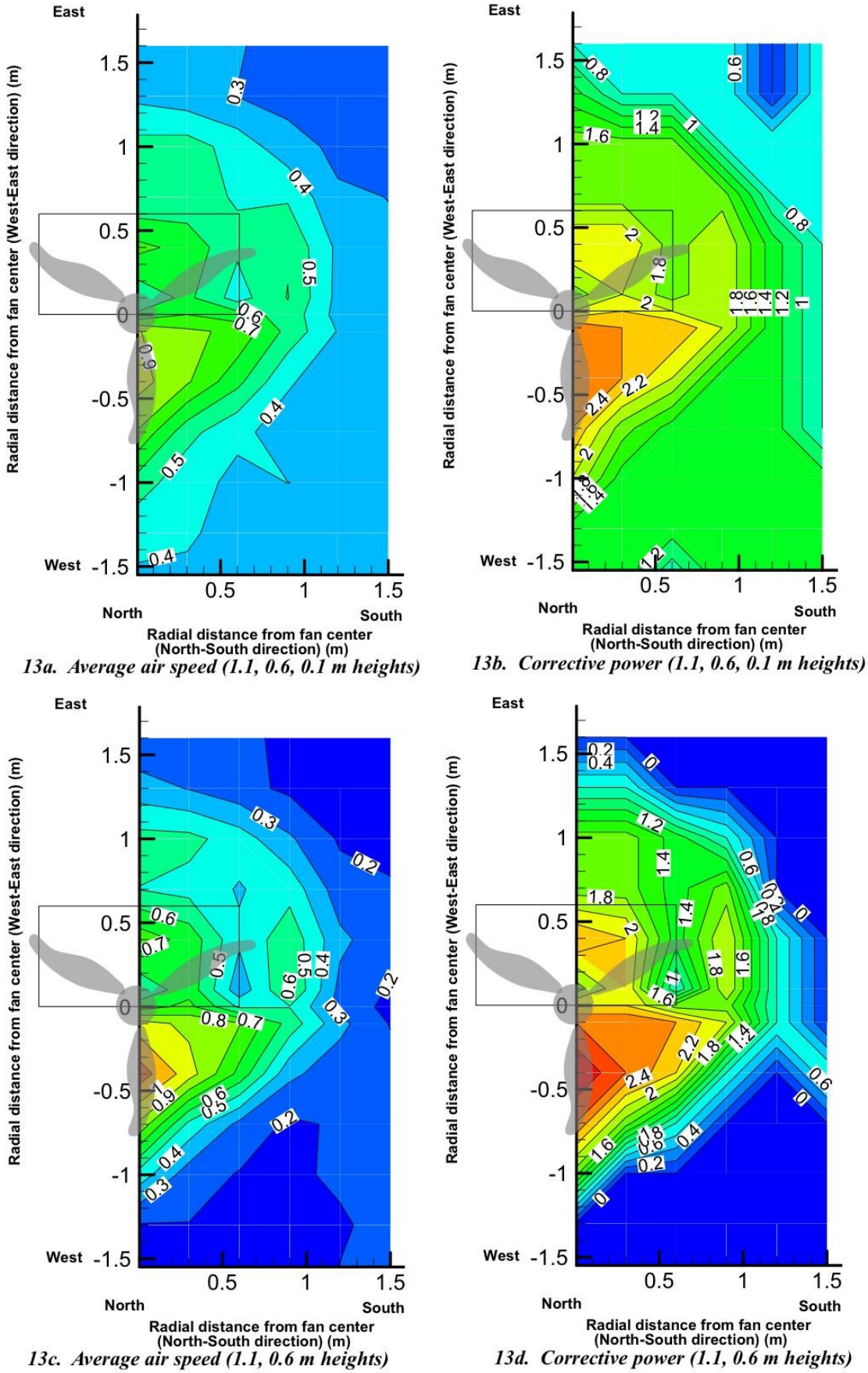

Figure 13: Average contours air speed and corrective power for three and two heights.

Comparing Figure 13 with the empty room case in Figure 7, the increased spread of higher velocities and corrective powers is clear, especially when the 0.1m air speed is not included in the average.

3.4 Case 4: Fan centered above table corner

Both Case 4 air flow profiles are similar to those of Cases 2 and 3, so they are not shown here. The spread beyond the table edge is very similar. However, because the table in Case 4 extends further beyond the diameter of the downward jet than other cases, it provides the greatest spread of higher speeds at the 0.75 and 0.6 m levels. This is seen in comparing the contour figures for Case 4 in the Appendix with those of other cases.

The placement of the fan above two corners of the table allows us to examine an aspect of swirl in the downward fan jet (Figure 14). In Case 4a the clockwise-directed swirl first encounters the short north edge of the table, and in Case 4b it encounters the long east edge. The air deflected across the table top and spilling from the edges differ in the two cases.

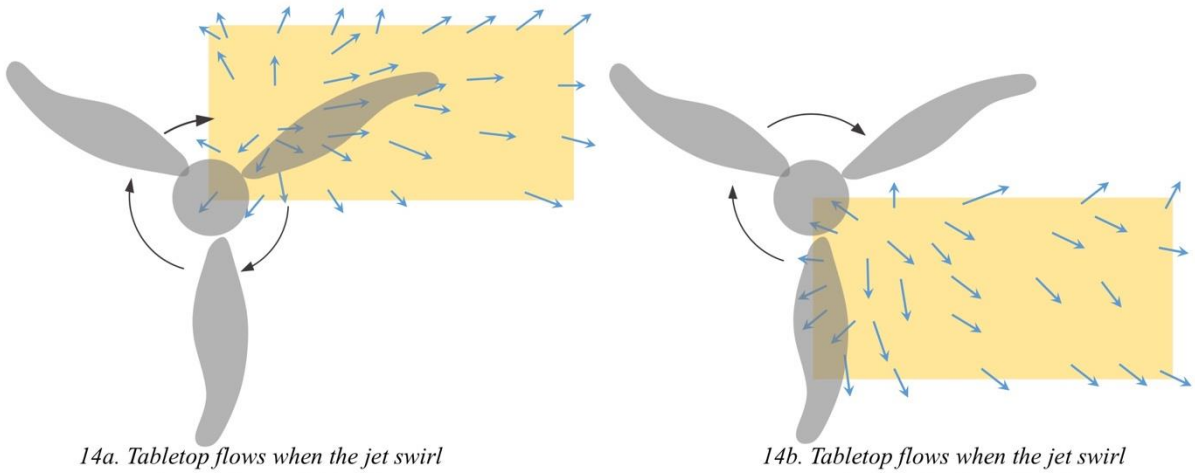

14a. Tabletop flows when the jet swirl approaches the longer table edge

14b. Tabletop flows when the jet swirl approaches the shorter table edge

Figure 14: Case 4 tabletop air flow directions from ceiling fan above two table positions.

Figures 14a and 14b show tabletop airflow patterns from the incense visualization tests. When the jet impinges on the table, it redirects the air flow outward along the table surface. A slight difference in pattern is seen between the two figures. The flow in 7b is directed somewhat more along the table length than in 7a, where it flows slightly more diagonally to the opposite corner of the table. In evaluating this, the air can be seen to be flowing away from a stagnation point occurring about 0.4 blade lengths from the hub. Within the circle of 0.4 radius, the stagnation point is located closer to the table's upwind edge (relative to the clockwise swirl) than to the table's center. This upwind offset of the stagnation point may be due to swirl in the downward jet. The effect is subtle and unlikely to require attention in placing fans and furniture in workstations.

3.5 Case 5: Fan centered above table long edge; linear partition opposite

Case 5 repeats Case 3 with a 1.4 m high partition along the east edge of the table. The fan jet impinges on the entire table surface and envelopes the central half of the partition. The

partition blocks spillage off the east edge of the table, diverting it off the other edges. The air speed profile along the centerline of the fan, table, and partition is shown in Figure 15.

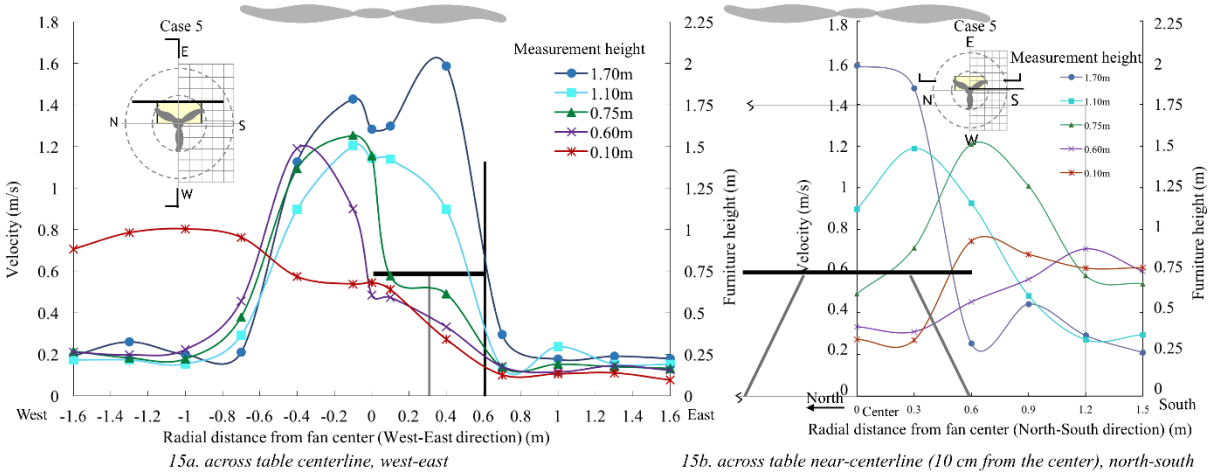

15a. across table centerline, west-east *15b. across table near-centerline (10 cm from the center), north-south*

Figure 15: Case 5 air speed profiles

As in Cases 2 and 3, the peak air speeds for 1.7, 1.1, and 0.75 m occur above the edge of the table, and for the 0.6 m height the peak occurs 0.4 m beyond the edge of the table. The partition diverts airflow most significantly off the ends of the table to north and south, whereas the downward jet in the occupied region to the west of the table suppresses the spread there (See the horizontal and vertical contours for Case 5 in the Appendix).

3.6 Case 6: Fan centered above table long edge; corner partition opposite

Figure 16: When the linear partition in Case 5 is folded to abut the northern table edge, it forms a corner partition. The air that was deflected towards the north side in Case 5 is blocked by this new partition and redirected towards the south-west quadrant, creating a more uniform air speed distribution within the workstation's occupied space than in any other case. Peak velocities at 1.7 m and 1.1 m occur 0.4 m from the fan center (also the edge of the table). The peaks at 0.75 m and 0.6 m height extend 0.7 m and 1.0 m beyond the table edge, and the air speeds in the occupied zone to the west and south of the table are much higher than that in case 5.

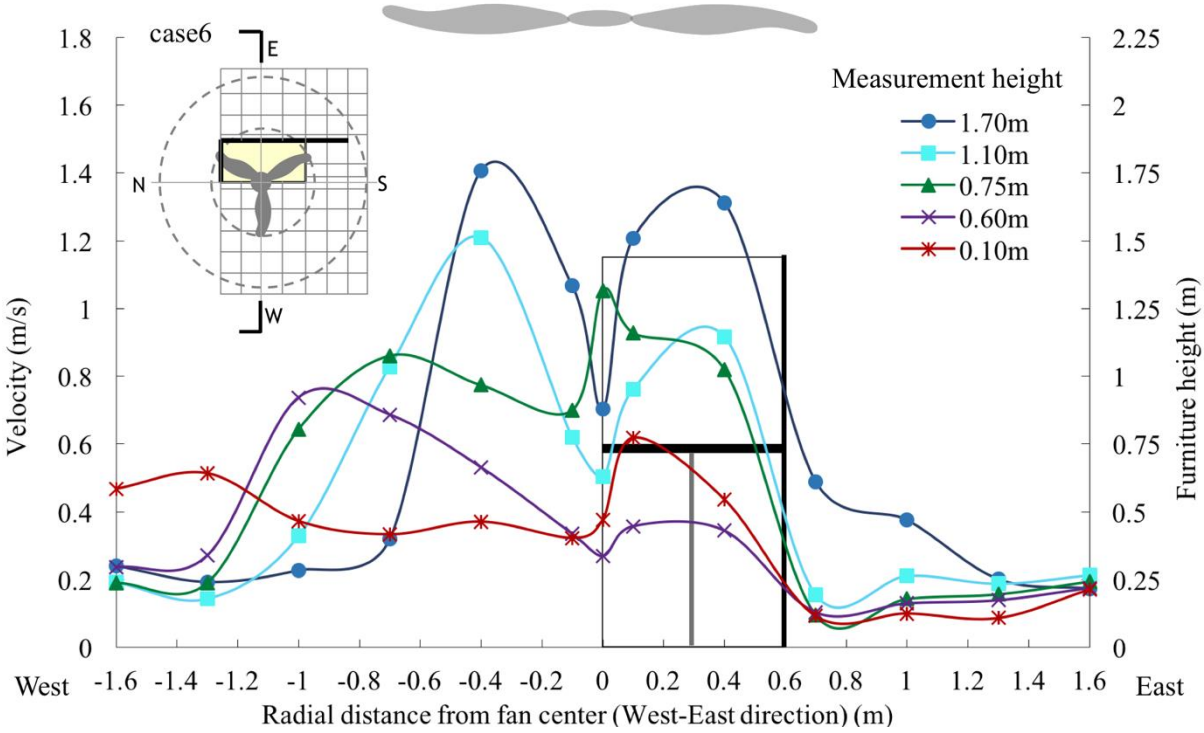

Figure 16: Case 6 air speed profiles along the fan centerline, west-east.

Vertical contours: The vertical air speed contours in the same section show the air flow spreading significantly in the west quadrant (Figure 17). Comparing these contours with those for the linear partition (Appendix Cases 5 and 6), Case 6 has much higher air speeds in the region further than 1m from the west table edge.

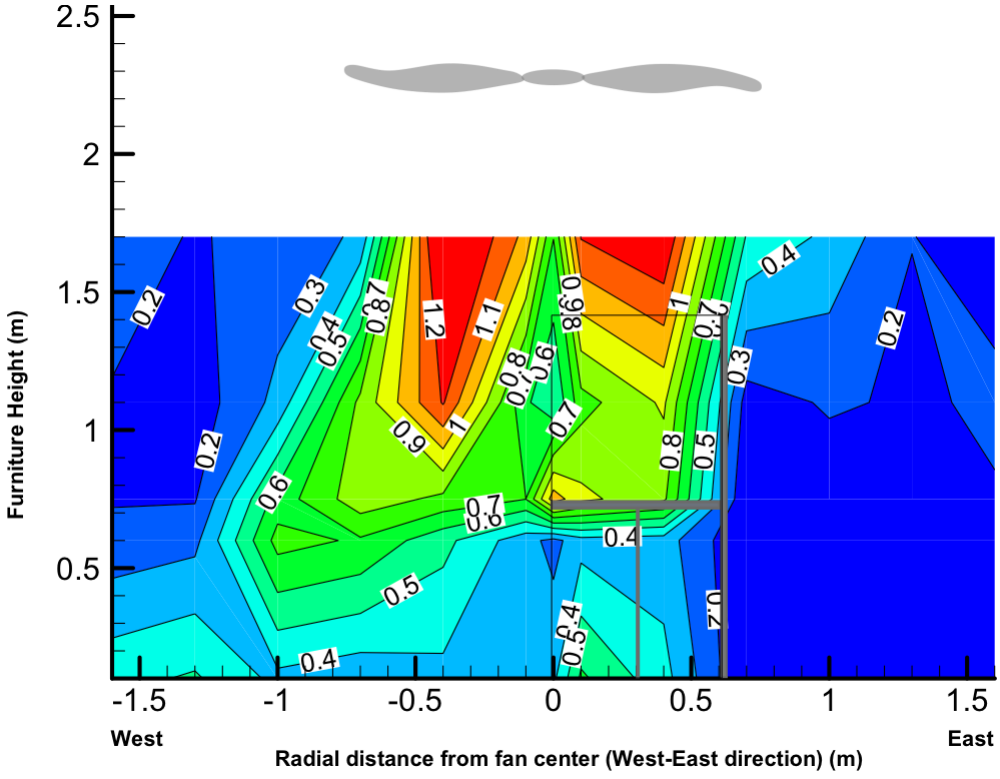

Figure 17. Vertical contour through center of fan (Case 6, C-0m)

Horizontal contours: Comparing all the tested heights, the corner partition created the most uniform air speed in the workstation for all heights except at 1.7 m (Figure 18). The enlarged air speed coverage area can also be seen in Table 3.

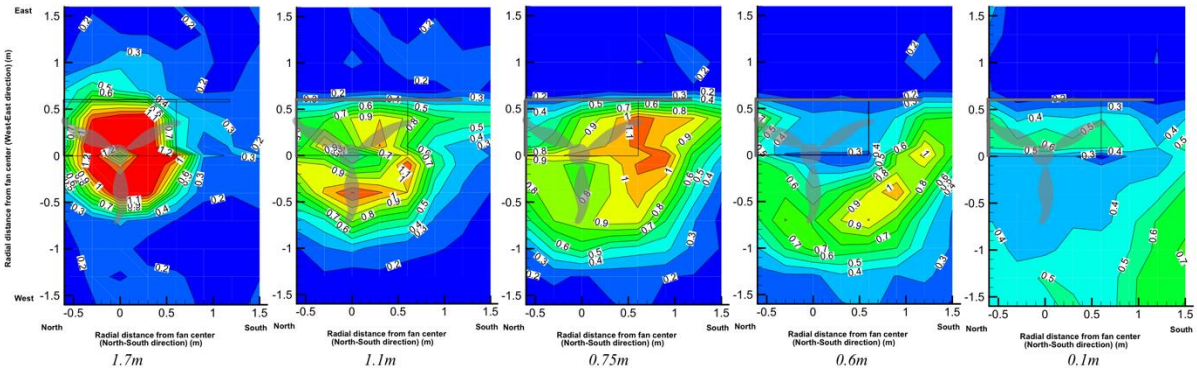

Figure 18: Horizontal contours for Case 6 corner partition workstation

Table 3: Flow spread area for different heights using 0.3 m/s as the threshold, Case 6

L-partition	1.7 m	1.1 m	0.75 m	0.6 m
Table and partition side	R_{south}=0.9 m V_{max}=1.5 m/s	R_{south}>1.5 m V_{max}=1.0 m/s	R_{south}>1.5 m V_{max}=0.9 m/s	R_{south}>1.5 m V_{max}=0.5 m/s
Non-table side	R_{west}=0.7 m R_{south}=0.9 m V_{max}=1.4 m/s	R_{west}=1.0 m R_{south}=1.5 m V_{max}=1.2 m/s	R_{west}=1.2 m R_{south}>1.5 m V_{max}=0.8 m/s	R_{west}=1.5 m R_{south}>1.5 m V_{max}=0.8 m/s

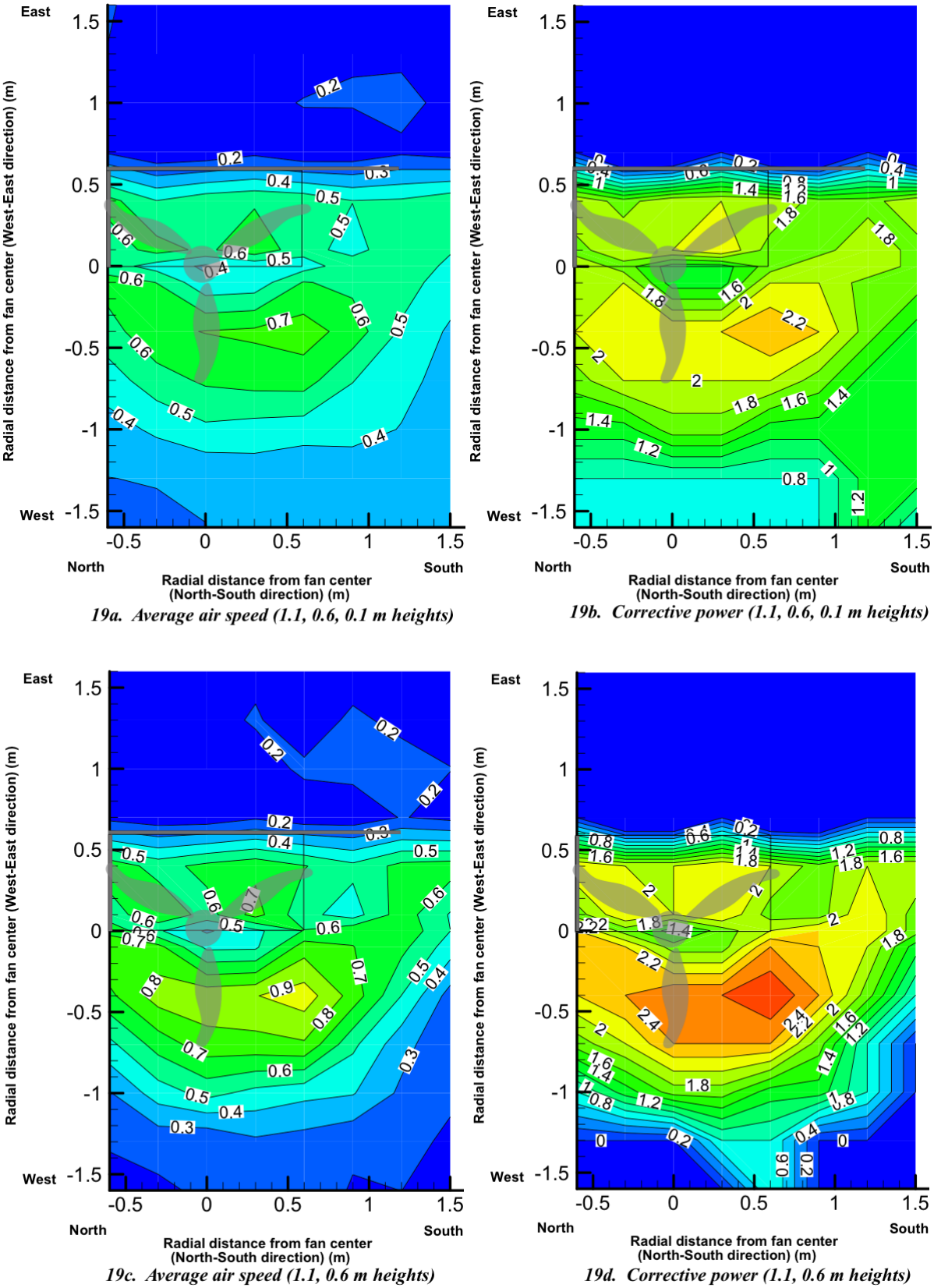

Figure 19: Contours of average speeds and corrective powers; Case 6.

Figure 19 a-d show the average air speeds available for cooling an occupant, and the comfort corrective power for the corner partition. The spread of the cooled region is greater than for the linear partition in Case 5. The region of cooling air speeds is also notably greater and more uniform than it is in the Case 1 empty room base case (also see Appendix).

4. Discussion

Describing ceiling fan flow as a jet flow.

These measured data can be compared with existing free-jet theory and with impingement jet theory [18][19][20]. Since the free-jet theory was developed for nozzle flows, some parameters that are important for ceiling fans, e.g. the non-uniformity of the jet velocity directly below the propeller blades, are not included in the jet theory studies mentioned above. More work would be needed to thoroughly categorize the ceiling fan using jet theory.

A ceiling fan jet is the sum of three components:

- Free jet, with a uniform potential core and entrainment occurring around the perimeter of the jet.
- A propeller produces a ring jet with a low-speed core below the hub. The core air speed fills in with distance downwind from the fan, and also with impingement against horizontal surfaces like floor or table. The perimeter entrainment for the propeller-driven ring jet appears to be similar to that of a pure free jet (figures 3) but details should differ.
- Propeller-imparted swirl adds a rotational component to the ring jet velocity [23].

  For a room air flow model, swirl might be dealt with three ways:

  - Neglected
  - Direction of rotation noted
  - Rotational velocity determined

  Rotational velocity was not measured in this study. Case 4 provides some insight into the effect of swirl direction on flows spreading off a table top. Swirl was seen to produce a small effect on the location of the stagnation point on the table top, and in the spreading distribution off the edges of the tabletop. For a simplified room air flow model these differences appear sufficiently small that swirl might be neglected. It might however be possible to use these results to develop a model of airflows and comfort around the edges of a table beneath a ceiling fan, in which swirl direction is a significant input parameter.

Developing a conceptual *model for ceiling fan placement within a room*

The material collected in this study is sufficient to propose a conceptual organizing model for ceiling fan airflow within a room, particularly the flows cooling the occupied zone, below 1.7 m above the floor (for standing occupants) or 1.1 m (for seated occupants). The effects of typical office furnishings must be included in the model since they have a strong effect on air flow and on the resulting occupant comfort. Almost all previous work on this topic has been in empty rooms.

For design purposes, it helps for this room model to be simplified to reveal memorable generic patterns in the air flow, and be a framework for understanding. The simplifications are:

- Jets originating from propeller ceiling fans are generic enough to be treated identically.

- The fan jet provides the momentum input to a simplified model of ceiling fan flows in a room.
- The model contains
    - the columnar fan jet
    - impingement zones where air flow encounters a surface and is forced to change direction (floor, wall, ceiling; tabletop, room partition, collision with contrary airflow),
    - zones of shallow depth along room and furniture surfaces (floor, walls, and tabletops within which air flow spreads or is channeled).
    - Everywhere else is effectively a still air zone whose overall upward flow is too slow to be perceptible.

These are shown in the following two figures. These are not drawn to exact scale, and do not correspond directly to the measured cases presented in this paper. Their patterns are however generalized from those measurements and from pilot tests. The 'empty room' figure shows the fan jet, the impingement zone directly below the fan, a spreading zone of equal thickness across the floor, another set of impingement zones at the base of the walls, and wall zones with upward flow. This pattern continues at the ceiling but as this is above the occupied zone it is not an issue here. (The main concern in the ceiling zone is that the fan is mounted a sufficient distance below the ceiling to avoid starving its inflowing air. This mounting depth should exceed 0.5 times the fan radius.) Note the small spots near the middle of each impingement zone. These are the stagnation points where impinging air speed is reduced to zero and air pressure is highest. Flows are diverted away from stagnation points. The rest of the space is the still air zone where the fan is not cooling the occupant.

An additional point about spreading zone on floor: the horizontal velocity diminishes with distance from the impingement zone due to circumferential spreading. This is seen in Figures 4 and 5. The flow does not behave as simple channel flow because of frictional losses along the solid boundary of the floor and to eddy entrainment along the still air zone boundary. In most practical situations, flows on the floor are channeled by furniture and become complex.

Figure 20 shows the effects of a typical table top on the impinging fan jet. It spreads the jet laterally and raises the depth of the spreading zone above the floor. These effects are desirable, as the distributed air flow more effectively cools occupants in the occupied zone, and produces less variable air speeds within the occupied zone. One can also visualize these effects as 'eating away' the size of the undesirable still-air zone. Measured data supporting this are seen in Cases 2-4.

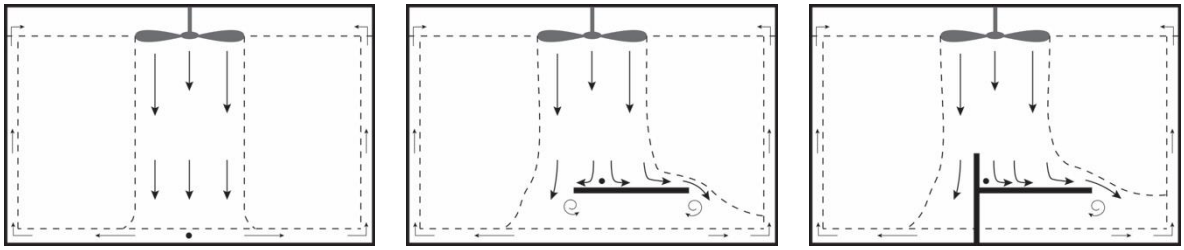

Empty room | With table | With table+partition

Figure 20: Room air flow circulation driven by a ceiling fan

The 'with-table-and-partition' figure shows that by vertically confining the impingement zone on the tabletop with a partition, the stagnation point moves to the left into the corner,

and the redirected flow traveling to the right across the table is increased. This pattern of trapping flows with a barrier parallel to the incoming air jet and redirecting them elsewhere is also conceptually generic and can be perceived intuitively by designers. Measured data in Cases 5 and 6 support this pattern. Another notable point is that the flow off the table top spills off the table edge in a shallow downward angle. The flow being isothermal, this is due to momentum effects and entrainment into the underlying room circulation.

Figure 21 shows that local impingement between spreading flows from multiple fans, or impingement against floor-mounted partitions, will cause vertical flows that also 'eat away at' the still air zone and improve the fan cooling near them. Multi-fan and floor-mounted partition effects were not tested in this study and will need additional study to quantify, but are generically observed patterns. The perpendicular outflow from colliding air streams has been quantified for unbounded free jets [24], [25].

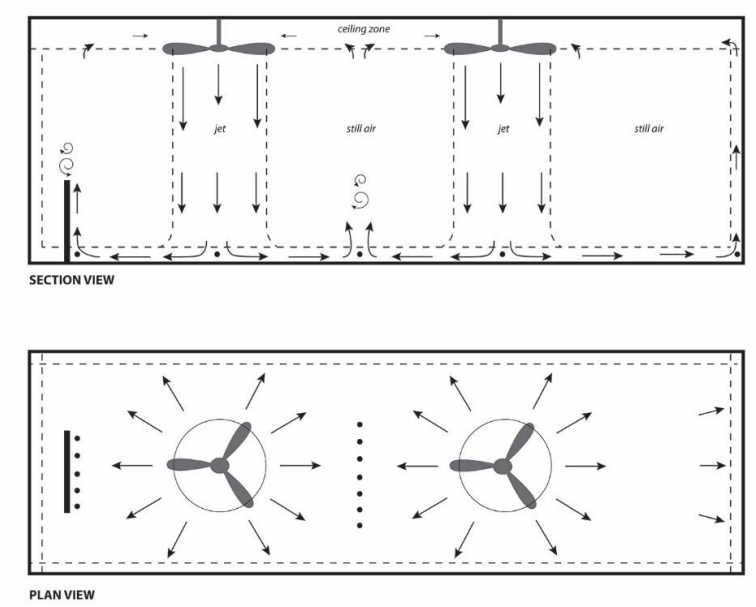

Figure 21 Room air flow circulation driven by multiple fans

Note that when low-speed momentum flows dissipate into viscosity, the hydraulic channel nature of the circulation implied in this model will break down. However, for design purposes it is most likely that we can focus on the range of speeds where momentum flow persists, at least as it passes through the occupied zone. In other words, we might assume that people will use the fan's higher speeds when cooling is needed, and circulation patterns that are breaking down need not be the focus of design.

To quantify some of the features of this conceptual model, we can use some of the measurements from this study:

Ceiling fan air flow in an empty room does not spread significantly until it descends to within a short distance above the floor. (For the fan size and height in this study, this was 0.3m-0.5 m above the floor, but for larger fan diameters and heights the depth of the impingement and spreading zone can be expected to increase). Within the fan jet there are peaks in a concentric ring of 0.75 blade diameter that diminish until they even out roughly 0.6 m above the floor.

When the fan jet impinges on a table, it spreads, pushing the air speed peak at table height (0.75 m) towards the edge of the table, and the peak at 0.6 m height about 0.4 m further outward from the table edge. In the table-plus-partition combinations, the peak speeds decrease, but the flow more uniformly covers a bigger area where occupants are located. The workstation with the corner partition on the table created the most uniform air flow of the cases considered.

It is significant for comfort that the spreading caused by impingement on the table has a small effect at the 1.1 m head height and above. The peak velocities within the jet occur further from fan center (0.2 to 0.4 m), but the jet area is small relative to the room area. The jet diameter itself is roughly the same as it is in the empty room. So the presence of the table does not appreciably increase the area in which the fan directly cools the head.

The spreading and air speed increases are occurring at the mid-body levels measured here (0.75 and 0.60 m), while the air speed at floor level (0.1 m) is decreased within the thickened spreading layer. Cooling increases as air speed increases around the mid-body with its much larger surface area than the ankles and feet. Since convective cooling is roughly proportional to the square root of air speed, the initial speed increases above 0.3 m/s are the most effective, e.g., 0.4 to 0.8 m/s. The comfort effects caused by this upward shift in localized cooling have not been addressed in the literature, although a study of ankle comfort under displacement ventilation provides preliminary insights [26]. Ultimately the cooling effects on the different body parts might be addressed by weighting the air speeds when averaging the three heights. The weighting could represent the relative body surface areas, clothing levels, and physiological sensitivity of the affected body parts. For now, we approximate the range of possible cooling effects by presenting corrective power in two forms: as a function of air speed averaged over three heights, and averaged over the upper two heights.

The following phenomena were not addressed in this study and subjects for subsequent studies: vertical obstructions that are perpendicular to the horizontal spreading flow on the floor and outside the area of the descending fan jet (note that the vertical partitions in this study are within the impingement zone of the fan jet and are therefore parallel to the incoming flow. There are two types of perpendicular obstructions:

- furniture partitions on the floor outside the fan jet diameter
- counterflow along the floor originating from a second fan

These each create a new stagnation point and impingement zone that redirects the flow upward into the still air zone. Unlike the upward flows along the room walls, this flow is unbounded and dissipates its momentum more rapidly into incoherent turbulence. But even if turbulent, the additional air movement is good for comfort and increases the comfort in the occupied zone.

This work ties in with current efforts to develop ceiling fan methods of test and design guidance. Existing energy efficiency testing standards (AMCA 230-99, Energy Star) [27] [28] focus on volumetric flow, not air speed. A new ASHRAE Standard (216, ceiling fan method of testing) is currently under development to directly characterize speeds produced by ceiling fans within a room [29]. The standard is also intended to include guidelines and tools for designers placing fans within a room, and for evaluating comfort of occupants in

fan-cooled spaces. The measured data in this paper provides fundamental understanding and supporting material for developing the guidelines and tools.

5. Conclusion

This study measured air speeds generated by a single ceiling fan in a room with and without furniture, focusing on how the air speeds likely affect occupant cooling in the occupied zone. Useful patterns are revealed and a conceptual organizing model of room flow is presented. Additional measurements will be needed to complete the model, especially for rooms with multiple fans, but this study represents a significant beginning covering the single-fan case.

The air flow jet from the tested ceiling fan has certain significant properties. It does not spread until it descends to within 0.3m-0.5m above the floor. At 0.6 m height and above, the air speed in the area within the fan blade diameter is high, and outside of the fan blade diameter it is low. The air speed profile in a vertical plane has two peaks which predominantly are located within the middle position of the fan blade, and the two peaks continue down to 0.6 m above the floor. These features are seen in all three fan power levels tested except that there is somewhat more spread at lowest fan speed levels.

When the airflow impinges on a table, it spreads along the table surface. The impingement takes place below the height of an occupant's head, so the airflow at 1.1 m above the floor is minimally affected by the table. The maximum air speed at table height (0.75 m) occurs very close to the edge of the table. The peak at the 0.6 m height occurs about 0.3m – 0.4 m outward of the table edge. The peak air speed values observed at these two heights are lower than without the table, but instead of the peaks occurring within the fan jet, they take place over a much greater area, making the air speed distribution in the occupied part of the room more uniform. Using 0.3 m/s as the threshold for useful cooling air speed, the coverage distance for the 0.75 m and 0.6 m height extends about 2 times the fan radius. When the fan is located at the corner of a table that is extending well outside the fan blade radius (Case 4), the table creates a more uniform air flow distribution into the occupied zone.

A vertical workstation partition attached to one table edge channels the impinging air flow and spreads it laterally, parallel to the partition, off the ends of the table. When such a linear partition is folded around the end of the table to form an L-shape partition, the impinging vertical and lateral air flow is trapped and directed back towards the quadrant formed by the partition, forming a uniform air speed distribution over almost all of the occupied space, extending for more than twice the fan radius from the west table edge.

The air speed near the floor is generally high in rooms with ceiling fans, but its efficiency at cooling the occupant is lower than at the 0.6 and 1.1 m heights where the body has more surface area. Local ankle comfort and its dependence on the occupant's whole-body thermal state has not yet been thoroughly investigated in the literature. To cover the range of possible effects, we present cooling corrective power in two ways, with and without the air speed at ankle level.

The appendix data (also available in digital form as supplementary material) can be used for room airflow model development and validation.

Acknowledgement: This work is supported by National Natural Science Foundation of China (Project No. 51308129), and the California Energy Commission (CEC) Electric Program Investment Change (EPIC), Grant Award #: EPC-16-013. The authors would like to express appreciation to Jessica Uhl (Center for the Built Environment, UC Berkeley) for creating Figures 20 and 21.

References

[1] ANSI/ASHRAE, Standard 55-2013 Thermal Environmental Conditions for Human Occupancy, (2013).
[2] M. Fountain, E.A. Arens, Air Movement and Thermal Comfort, ASHRAE J. 35 (1993) 26–30.
[3] W. Pasut, E. Arens, H. Zhang, Y. Zhai, Enabling energy-efficient approaches to thermal comfort using room air motion, Build. Environ. 79 (2014) 13–19. doi:10.1016/j.buildenv.2014.04.024.
[4] Y. Zhai, H. Zhang, Y. Zhang, W. Pasut, E. Arens, Q. Meng, Comfort under personally controlled air movement in warm and humid environments, Build. Environ. 65 (2013) 109–117. doi:10.1016/j.buildenv.2013.03.022.
[5] S. Schiavon, A.K. Melikov, Energy saving and improved comfort by increased air movement, Energy Build. 40 (2008) 1954–1960. doi:10.1016/j.enbuild.2008.05.001.
[6] T. Hoyt, E. Arens, H. Zhang, Extending air temperature setpoints: Simulated energy savings and design considerations for new and retrofit buildings, Build. Environ. 88 (2015) 89–96. doi:10.1016/j.buildenv.2014.09.010.
[7] H. Zhang, E. Arens, Y. Zhai, A review of the corrective power of personal comfort systems in non-neutral ambient environments, Build. Environ. 91 (2015) 15–41. doi:10.1016/j.buildenv.2015.03.013.
[8] H. Zhang, E. Arens, S.A. Fard, C. Huizenga, G. Paliaga, G. Brager, L. Zagreus, Air movement preferences observed in office buildings, Int. J. Biometeorol. 51 (2007) 349–360. doi:10.1007/s00484-006-0079-y.
[9] E. Arens, S. Turner, H. Zhang, G. Paliaga, Moving air for comfort, ASHRAE J. (2009). http://escholarship.org/uc/item/6d94f90b (accessed January 13, 2017).
[10] J. Toftum, Air movement--good or bad?, Indoor Air. 14 Suppl 7 (2004) 40–45. doi:10.1111/j.1600-0668.2004.00271.x.
[11] F.H. Rohles, S.A. Konz, B.W. Jones, Ceiling fans as extenders of the summer comfort envelope, (1983). http://citeseerx.ist.psu.edu/viewdoc/download?doi=10.1.1.258.6085&rep=rep1&type=pdf (accessed November 21, 2016).
[12] Y. Zhai, Y. Zhang, H. Zhang, W. Pasut, E. Arens, Q. Meng, Human comfort and perceived air quality in warm and humid environments with ceiling fans, Build. Environ. 90 (2015) 178–185. doi:10.1016/j.buildenv.2015.04.003.
[13] J. Sonne, D. Parker, Measured ceiling fan performance and usage patterns: implications for efficiency and comfort improvement, in: ACEEE Summer Study Energy Effic. Build., Citeseer, 1998: pp. 335–341. http://citeseerx.ist.psu.edu/viewdoc/download?doi=10.1.1.626.2080&rep=rep1&type=pdf (accessed November 21, 2016).
[14] A. Jain, R.R. Upadhyay, S. Chandra, M. Saini, S. Kale, Experimental investigation of the flow field of a ceiling fan, in: ASME 2004 Heat TransferFluids Eng. Summer Conf.,

American Society of Mechanical Engineers, 2004: pp. 93–99. http://proceedings.asmedigitalcollection.asme.org/proceeding.aspx?articleid=1624779 (accessed November 21, 2016).
[15] R. Bassiouny, N.S. Korah, Studying the features of air flow induced by a room ceiling-fan, Energy Build. 43 (2011) 1913–1918. doi:10.1016/j.enbuild.2011.03.034.
[16] S.H. Ho, L. Rosario, M.M. Rahman, Thermal comfort enhancement by using a ceiling fan, Appl. Therm. Eng. 29 (2009) 1648–1656. doi:10.1016/j.applthermaleng.2008.07.015.
[17] D.G. Scheatzle, H. Wu, J. Yellott, Extending the summer comfort envelope with ceiling fans in hot, arid climates, ASHRAE Trans. 95 (1989).
[18] S. Beltaos, N. Rajaratnam, PLANE TURBULENT IMPINGING JETS, J. Hydraul. Res. 11 (1973) 29–59. doi:10.1080/00221687309499789.
[19] N. Rajaratnam, Turbulent Jets, Elsevier, 1976.
[20] P. Bradshaw, E.M. Love, The normal impingement of a circular air jet on a flat surface, HM Stationery Office, 1961. http://naca.central.cranfield.ac.uk/reports/arc/rm/3205.pdf (accessed April 21, 2017).
[21] Center for the Built Environment, CBE Thermal Comfort Tool for ASHRAE-55, (n.d.). http://comfort.cbe.berkeley.edu/ (accessed April 19, 2017).
[22] L. Huang, E. Arens, H. Zhang, Y. Zhu, Applicability of whole-body heat balance models for evaluating thermal sensation under non-uniform air movement in warm environments, Build. Environ. 75 (2014) 108–113. doi:10.1016/j.buildenv.2014.01.020.
[23] N.A. Chigier, A. Chervinsky, Experimental Investigation of Swirling Vortex Motion in Jets, J Appl Mech Trans Set E. 34 (1967) 443–451.
[24] C. Liu, H. Higuchi, E. Arens, H. Zhang, Study of a Personal Environmental Control System Using Opposing Airstreams, Proc. Indoor Air 2011. (2011). http://escholarship.org/uc/item/1jz8260r (accessed April 21, 2017).
[25] C. Liu, H. Higuchi, E. Arens, H.P.D. Zhang, Control of the microclimate around the head with opposing jet local ventilation, Cent. Built Environ. (2009). http://escholarship.org/uc/item/81d4s6gn (accessed April 21, 2017).
[26] S. Liu, S. Schiavon, A. Kabanshi, W.W. Nazaroff, Predicted Percentage Dissatisfied with Ankle Draft, Indoor Air. (2016). doi:10.1111/ina.12364.
[27] ANSI/AMCA, ANSI/AMCA Standard 230-2015 Laboratory Methods of Testing Air Circulator Fans for Rating, (2015).
[28] The US Environmental Protection Agency, Hunter Fan Company, Intertek Testing Services, ETL SEMKO, Underwriters Laboratory, Taiwan Branch, ENERGY STAR Testing Facility Guidance Manual: The Solid State Test Method for ENERGY STAR Qualified Ceiling Fans Version 1.0, (2002).
[29] C. Taber, Circulator Fan Performance Testing Standards, ASHRAE J. 57 (2015) 28.

Appendix A: Full set of figures for the 6 cases

Appendix A-1. Case 1: Base case, no furniture

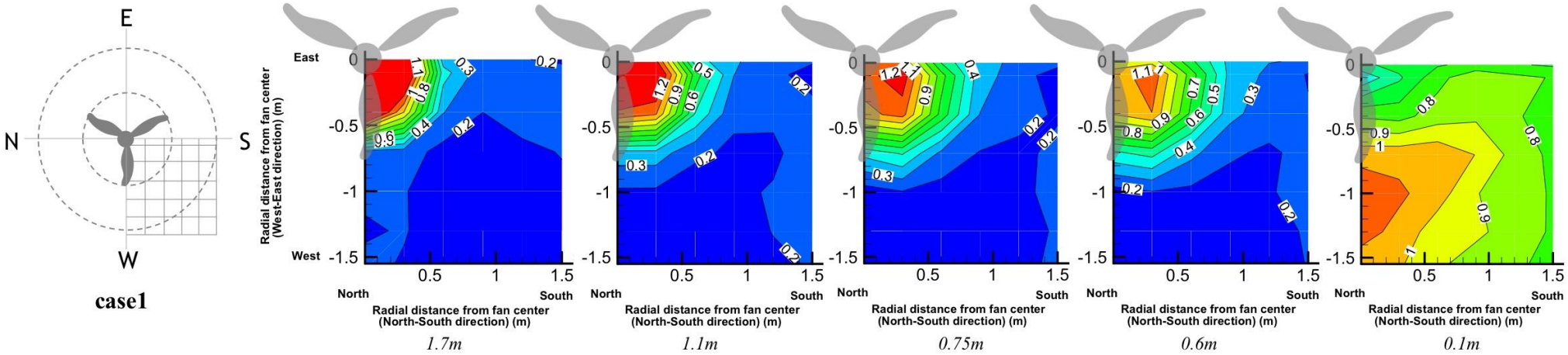

Case 1, Horizontal contours at all heights: 1.7m, 1.1m, 0.75m, 0.6m and 0.1m

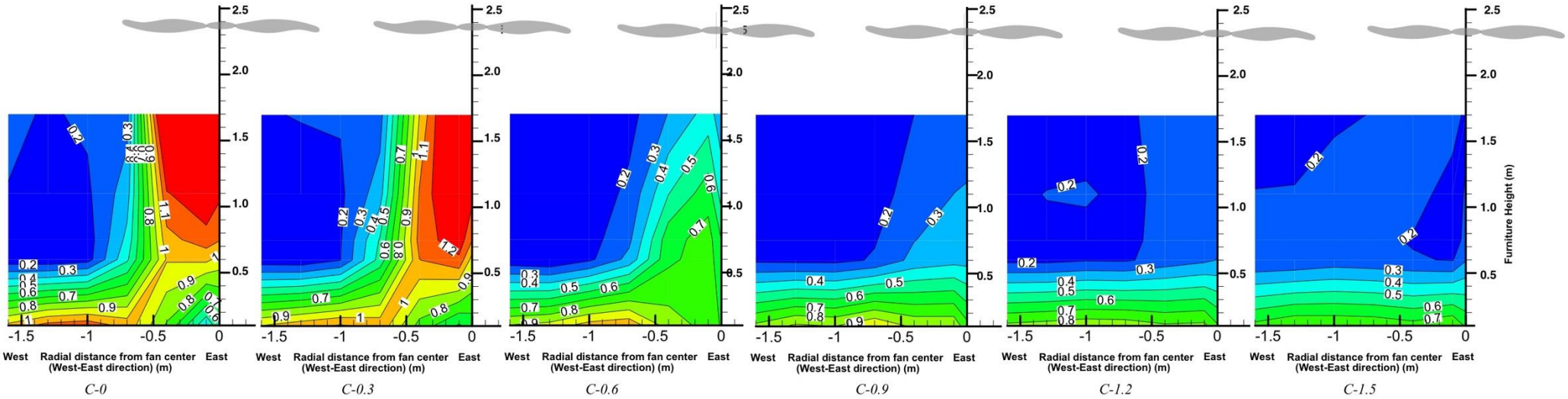

Caes 1, Vertical contours through all column positions:C-0,C-0.3,C-0.6,C-0.9,C-1.2 and C-1.5

Appendix A-2. Case 2: Fan centered above table midpoint

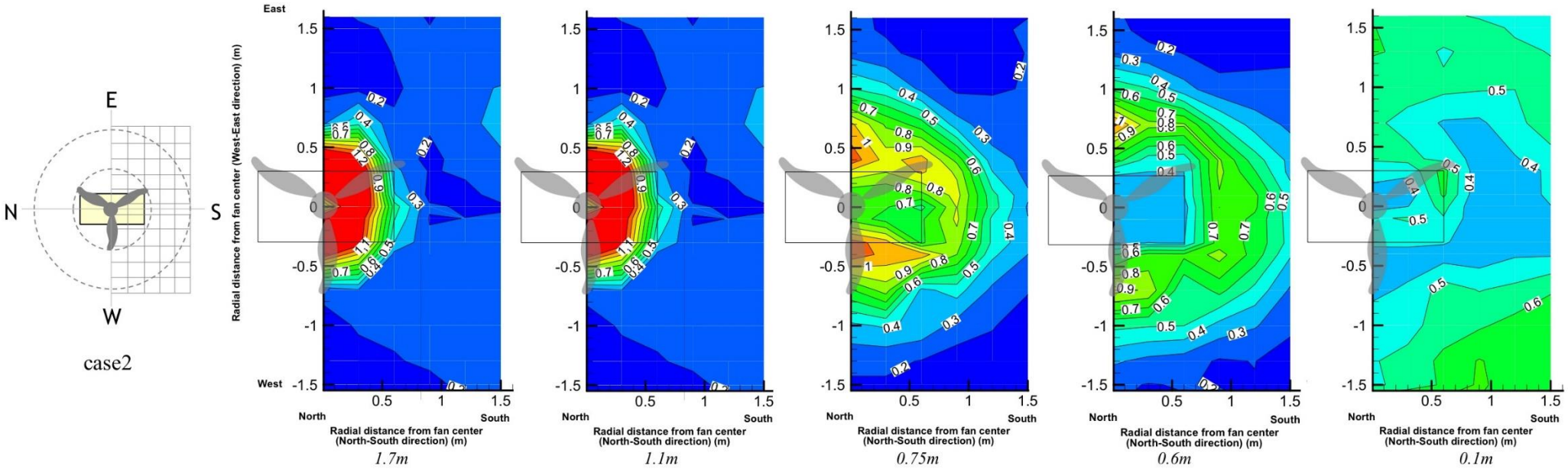

Case 2, Horizontal contours at all heights: 1.7m, 1.1m, 0.75m, 0.6m and 0.1m

APP-Table1: Flow spread area for different heights using 0.3 m/s as the threshold, Case 2

Case 2	1.7 m	1.1 m	0.75 m	0.6 m
Table under fan	R_{east}=0.7 m R_{south}=0.8 m R_{west}=0.7 m Vmax=1.6 m/s	R_{east}=1.1 m R_{south}=1.1 m R_{west}=1.0m Vmax=1.4 m/s	R_{east}=1.2m R_{south}=1.5 m R_{west}=1.2m Vmax=1.2m/s	R_{east}=1.3 m R_{south}=1.5 m R_{west}=1.3 m Vmax=1.1 m/s

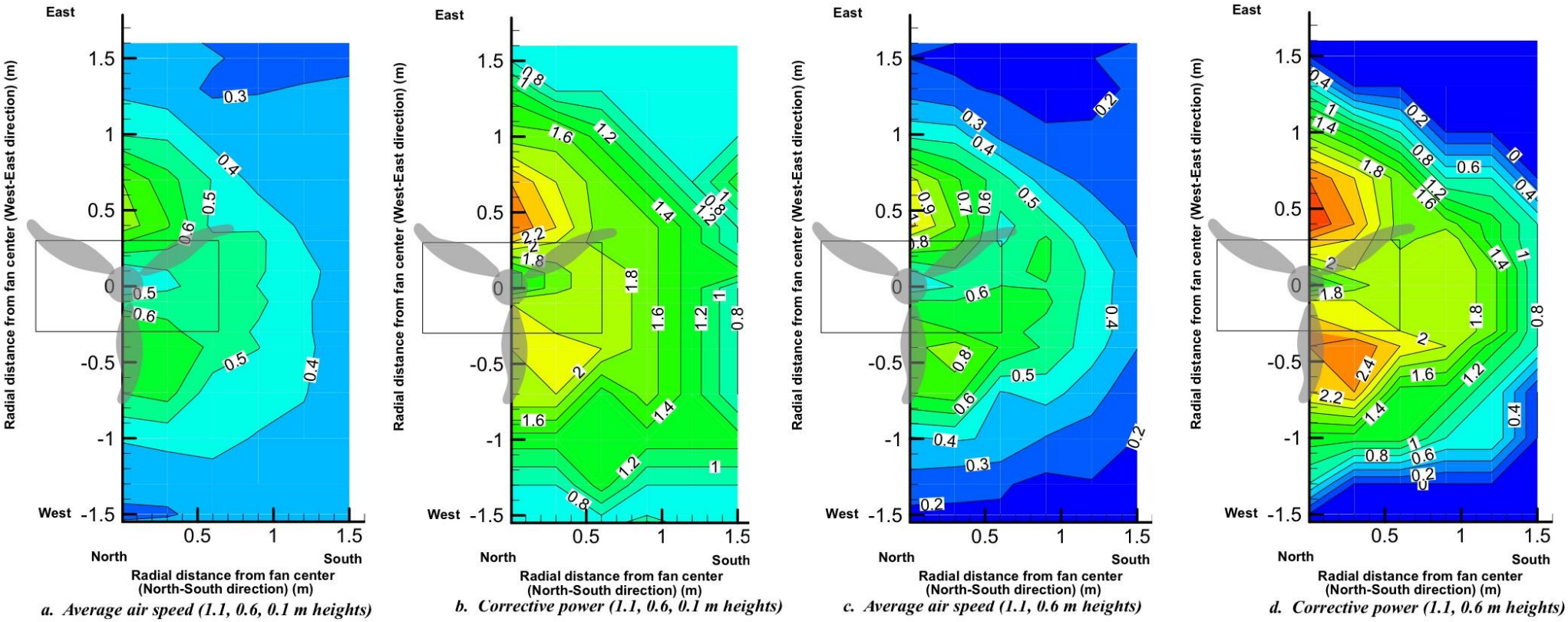

Caes 2, Contours of average speeds and corrective powers

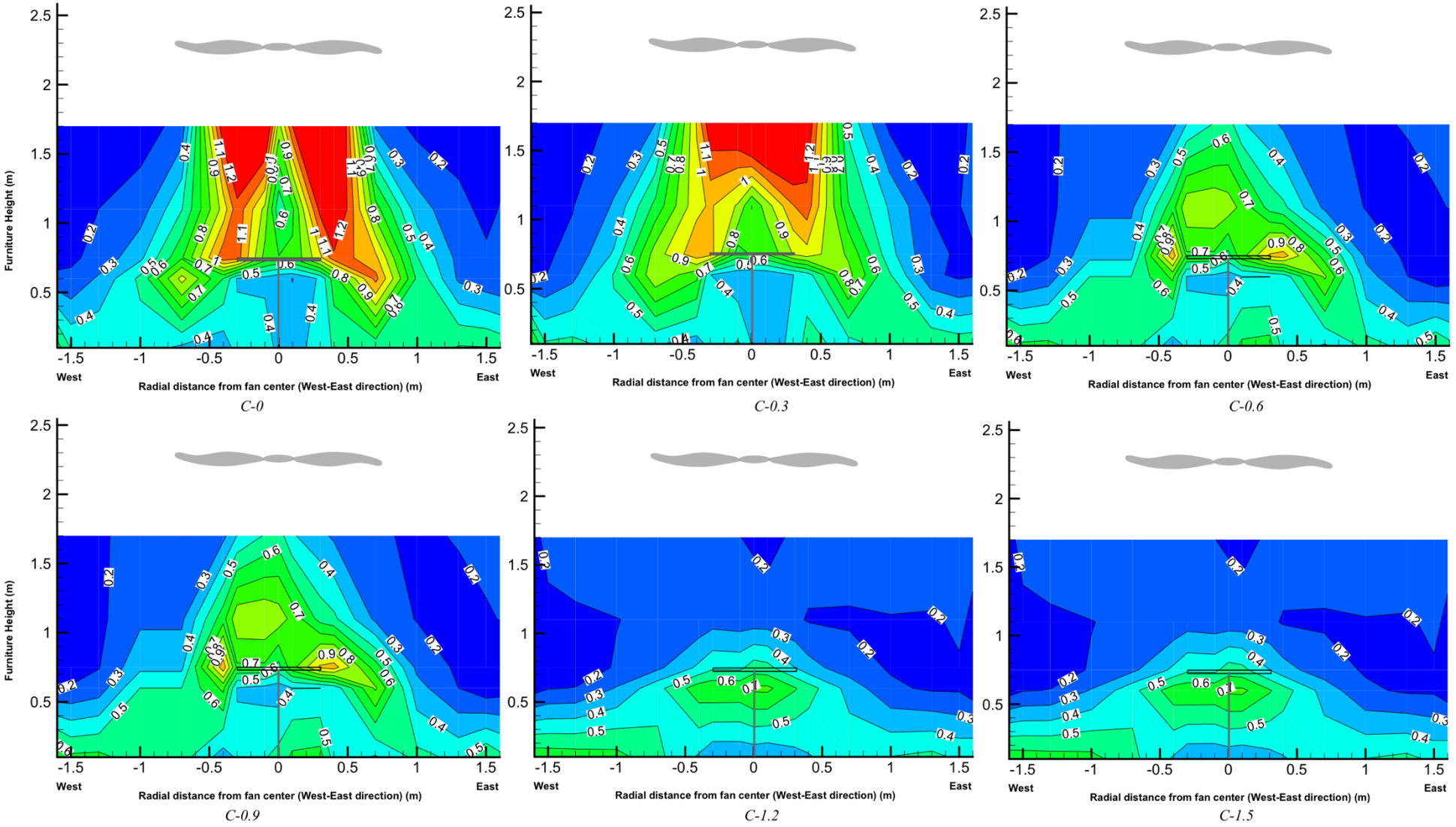

Caes 2, Vertical contours through all column positions:C-0,C-0.3,C-0.6,C-0.9,C-1.2 and C-1.5

Appendix A-3: Case 3: Fan centered above table long edge

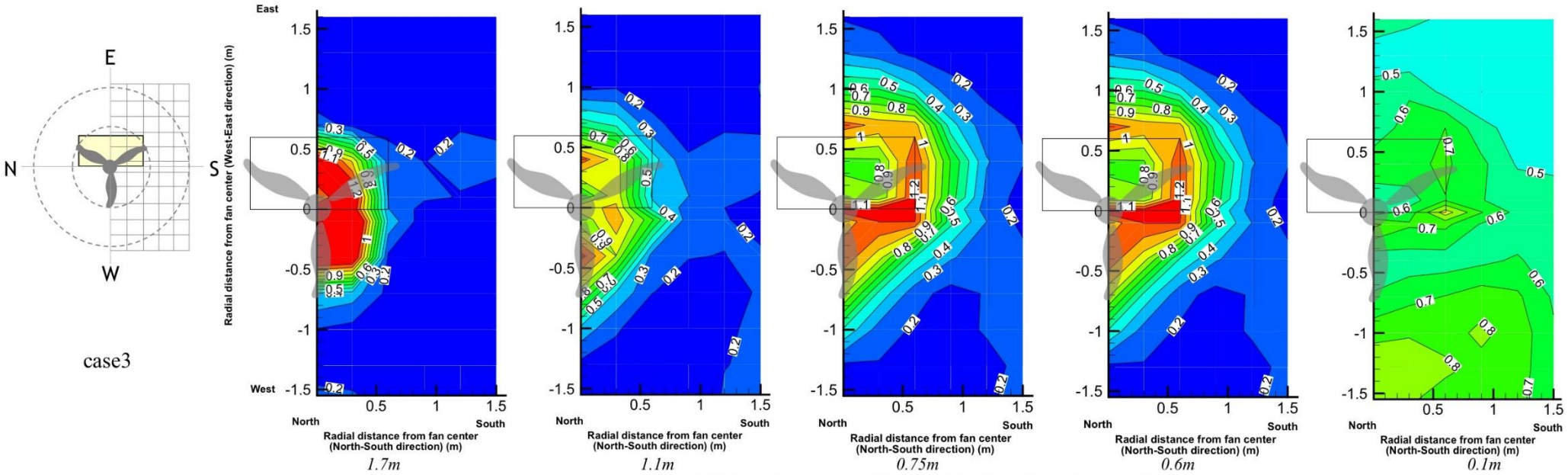

Case 3, Horizontal contours at all heights: 1.7m, 1.1m, 0.75m, 0.6m and 0.1m

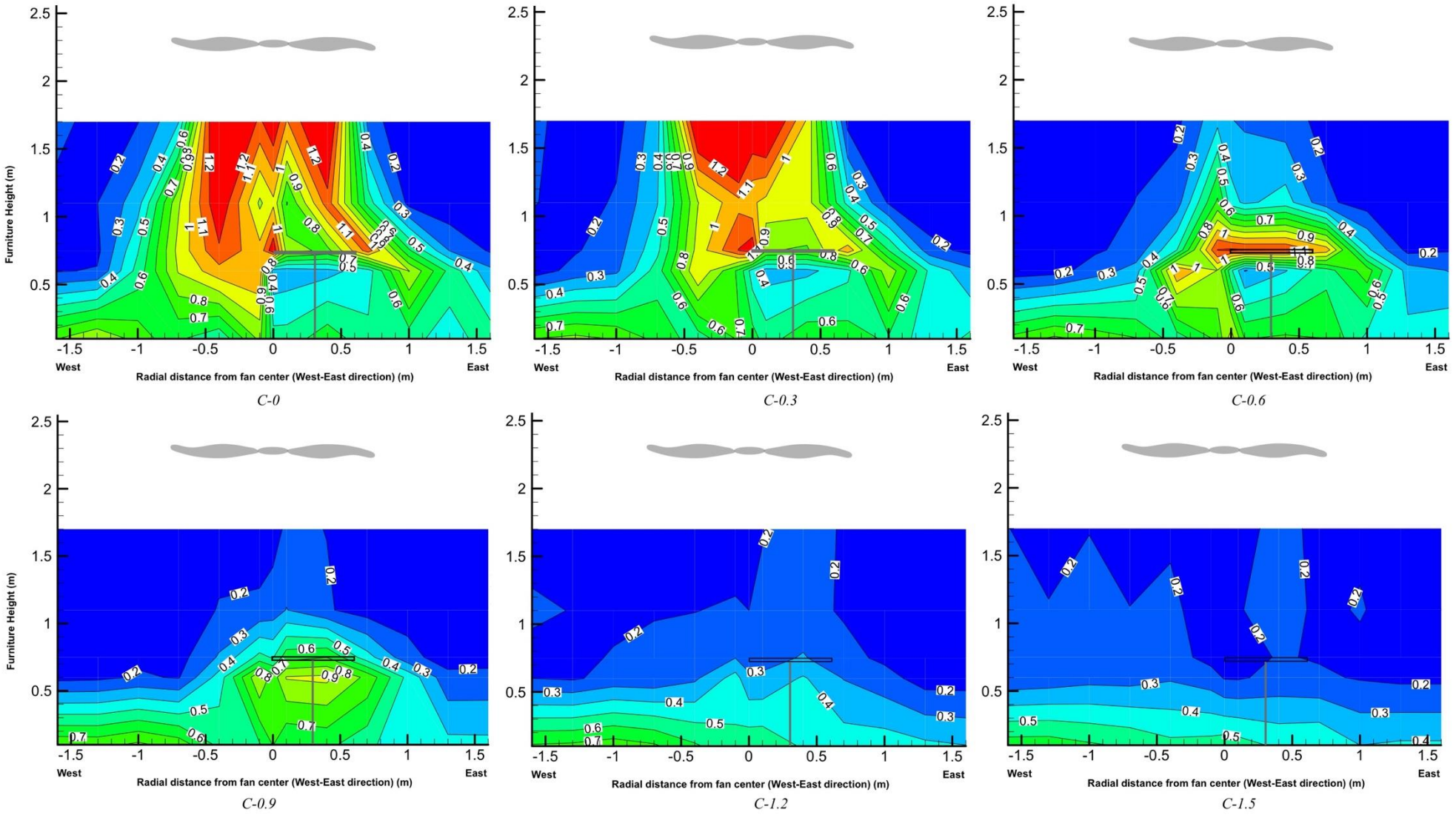

Caes 3, Vertical contours through all column positions:C-0,C-0.3,C-0.6,C-0.9,C-1.2 and C-1.5

Appendix A-4a. Case 4a: Fan centered above table corner

A: Table at south-east quadrant

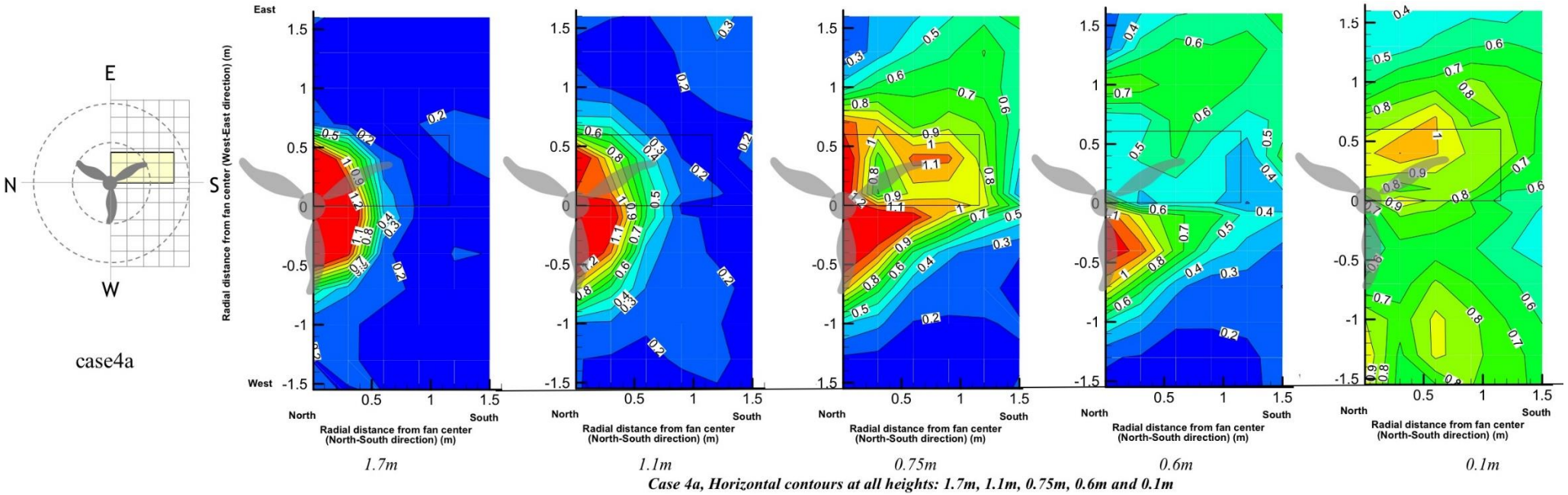

Case 4a, Horizontal contours at all heights: 1.7m, 1.1m, 0.75m, 0.6m and 0.1m

APP-Table 2: Flow spread area for different heights using 0.3 m/s as the threshold, Case 4a

Table at east-south quadrant	1.7 m	1.1 m	0.75 m	0.6 m
Table side	R_{west}=0.7 m R_{south}=0.6 m Quarter circle area V_{max}=1.7 m/s	R_{west}=0.9 m R_{south}=0.9 m Quarter circle area V_{max}=1.4 m/s	R_{west}>1.5 m R_{south}>1.5 m Rectangular area>2R*2R V_{max}=1.4 m/s	R_{west}>1.5 m R_{south}>1.5 m Rectangular area>2R*2R V_{max}=0.8m/s
Flow side	R_{south}=0.6 m R_{east}=0.9 m Quarter circle area	R_{south}=0.8 m R_{east}=1.0 m Quarter circle area	R_{south}>1.5 m R_{east}=1.2 m Triangle=1/2*2R*2R	R_{south}>1.5 m R_{east}=1.2 m Triangle=1/2*2R*2R

	V_{max}=1.6 m/s	V_{max}=1.6 m/s	V_{max}=1.4 m/s	V_{max}=1.3 m/s

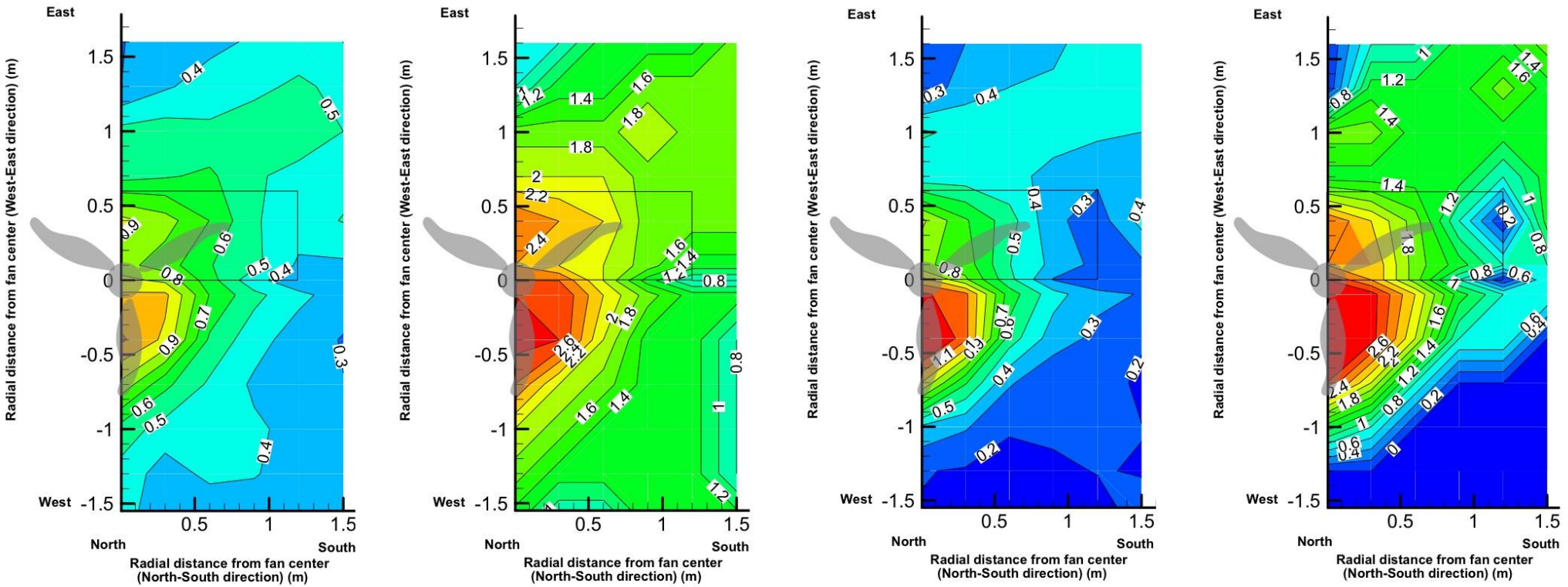

a. Average air speed (1.1, 0.6, 0.1 m heights)

b. Corrective power (1.1, 0.6, 0.1 m heights)

c. Average air speed (1.1, 0.6 m heights)

d. Corrective power (1.1, 0.6 m heights)

Caes 4a, Contours of average speeds and corrective powers

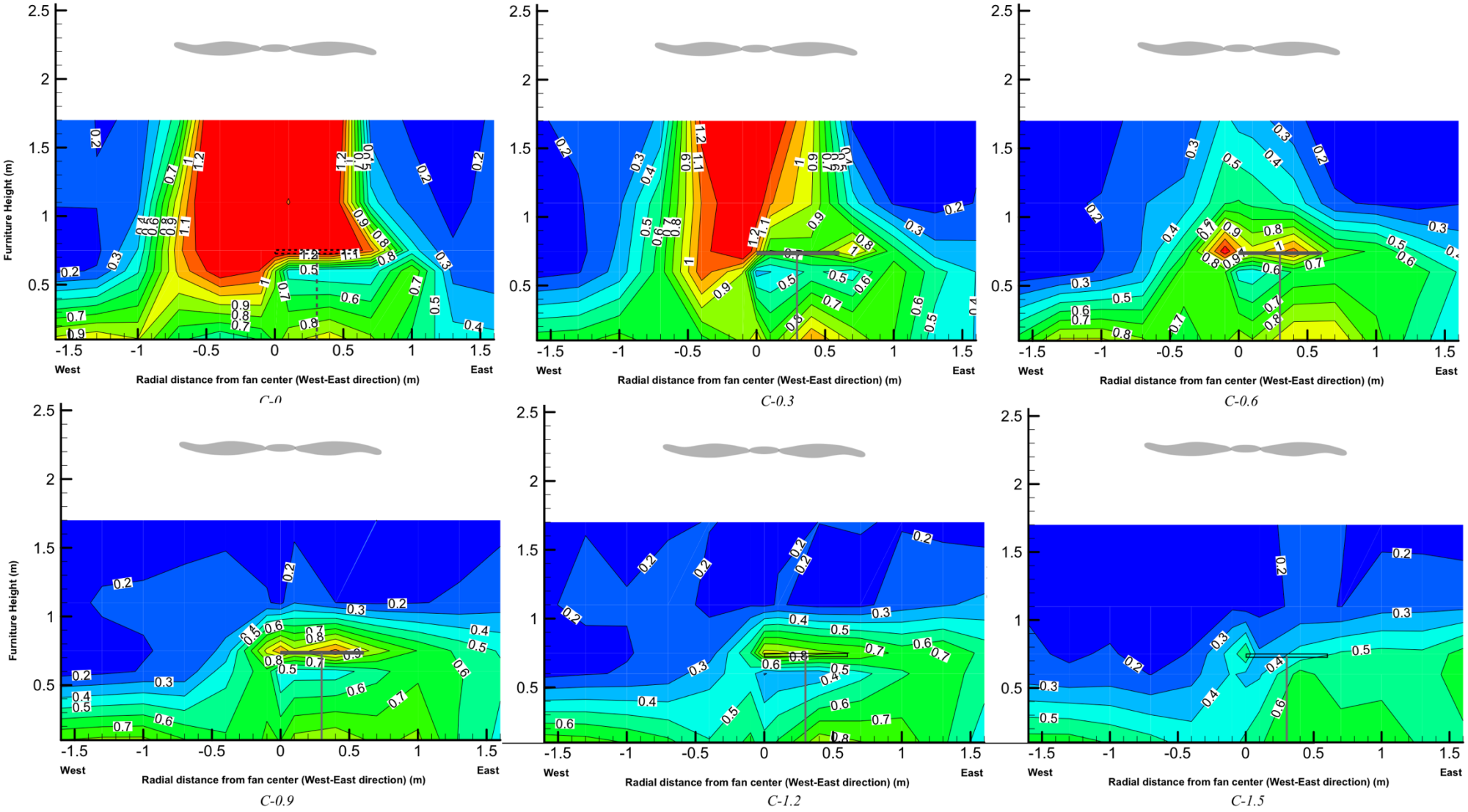

Caes 4a, Vertical contours through all column positions:C-0,C-0.3,C-0.6,C-0.9,C-1.2 and C-1.5

Appendix A-4b. Case 4b: Fan centered above table corner

B: Table at south-west quadrant

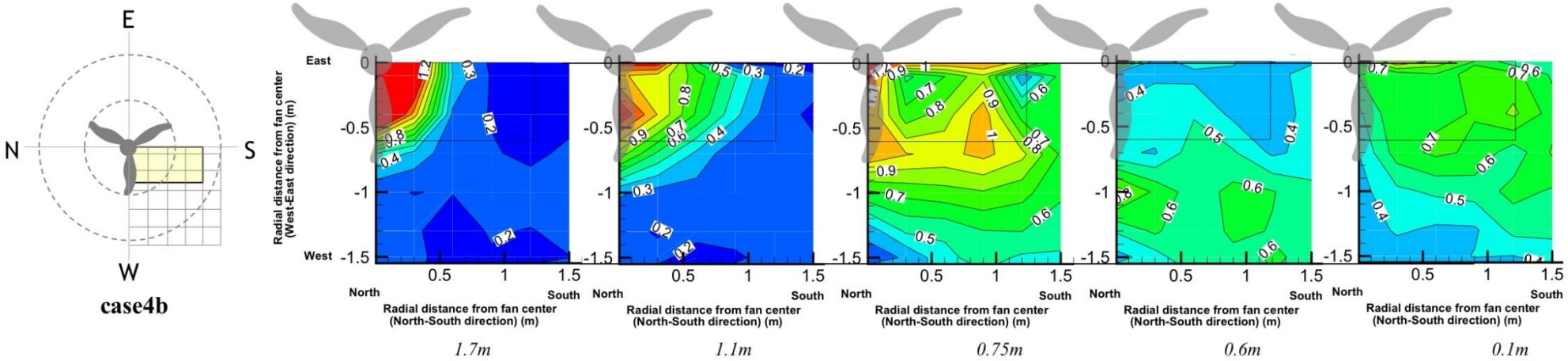

Case 4b, Horizontal contours at all heights: 1.7m, 1.1m, 0.75m, 0.6m and 0.1m

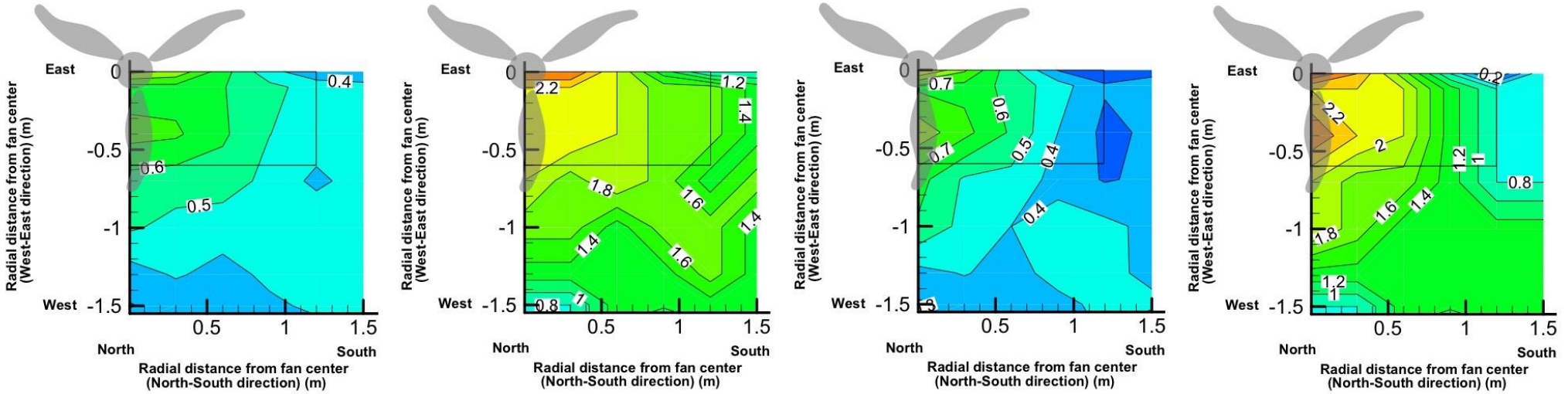

a. Average air speed (1.1, 0.6, 0.1 m heights) *b. Corrective power (1.1, 0.6, 0.1 m heights)* *c. Average air speed (1.1, 0.6 m heights)* *d. Corrective power (1.1, 0.6 m heights)*

Caes 4b, Contours of average speeds and corrective powers

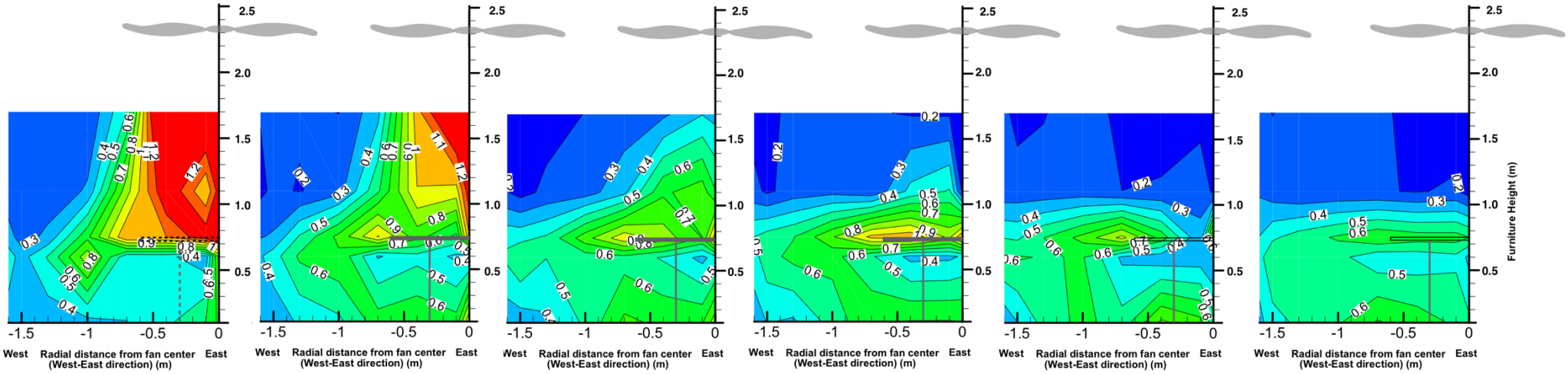

C-0 *C-0.3* *C-0.6* *C-0.9* *C-1.2* *C-1.5*

Caes 4b, Vertical contours through all column positions:C-0,C-0.3,C-0.6,C-0.9,C-1.2 and C-1.5

Appendix A-5. case 5: Fan centered above table long edge; linear partition opposite

http://doi.org/10.1016/j.buildenv.2017.08.029
www.escholarship.org/uc/item/3pq2j9mh

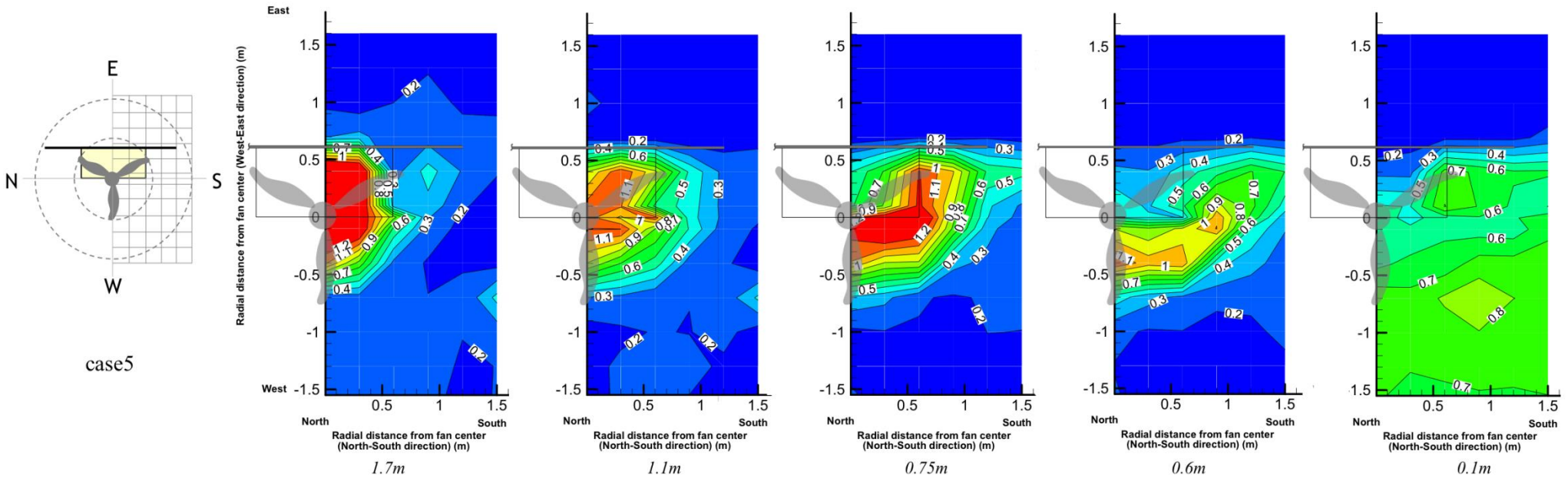

Case 5, Horizontal contours at all heights: 1.7m, 1.1m, 0.75m, 0.6m and 0.1m

APP-Table 3: Flow spread area for different heights using 0.3 m/s as the threshold, Case 5

Line partition	1.7 m	1.1 m	0.75 m	0.6 m
Southwest side	R_{south}=0.6 m, partly to 1.0m V_{max}=1.6 m/s	R_{south}=1.1 m V_{max}=1.1 m/s	R_{south}>1.5 m V_{max}=0.6 m/s	R_{south}>1.5 m V_{max}=0.5m/s
Southeast side	R_{west}=0.65m R_{south}=0.9m V_{max}=1.4 m/s	R_{west}=0.7 m R_{south}=1.1 m V_{max}=1.2 m/s	R_{west}=0.8 m R_{south}=1.4 m V_{max}=1.3 m/s	R_{west}=0.8 m R_{south}>1.5 m V_{max}=1.2 m/s

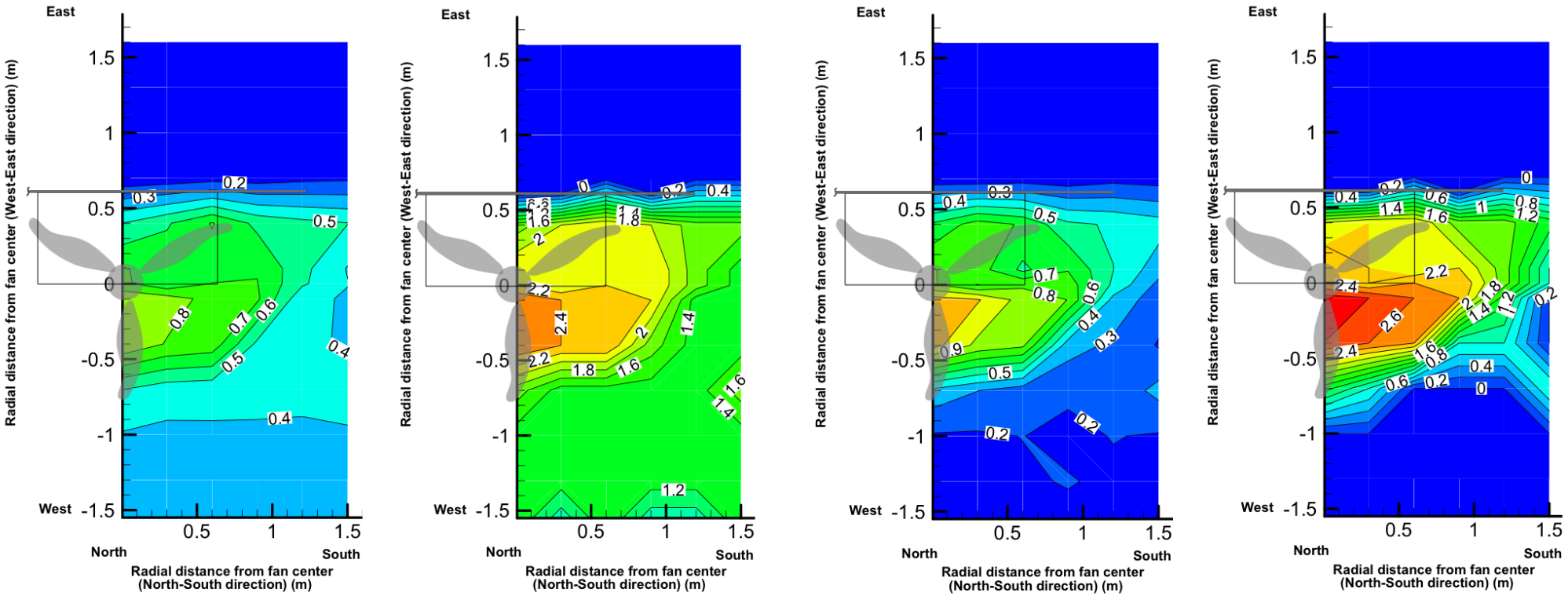

a. Average air speed (1.1, 0.6, 0.1 m heights) *b. Corrective power (1.1, 0.6, 0.1 m heights)* *c. Average air speed (1.1, 0.6 m heights)* *d. Corrective power (1.1, 0.6 m heights)*

Caes 5, Contours of average speeds and corrective powers

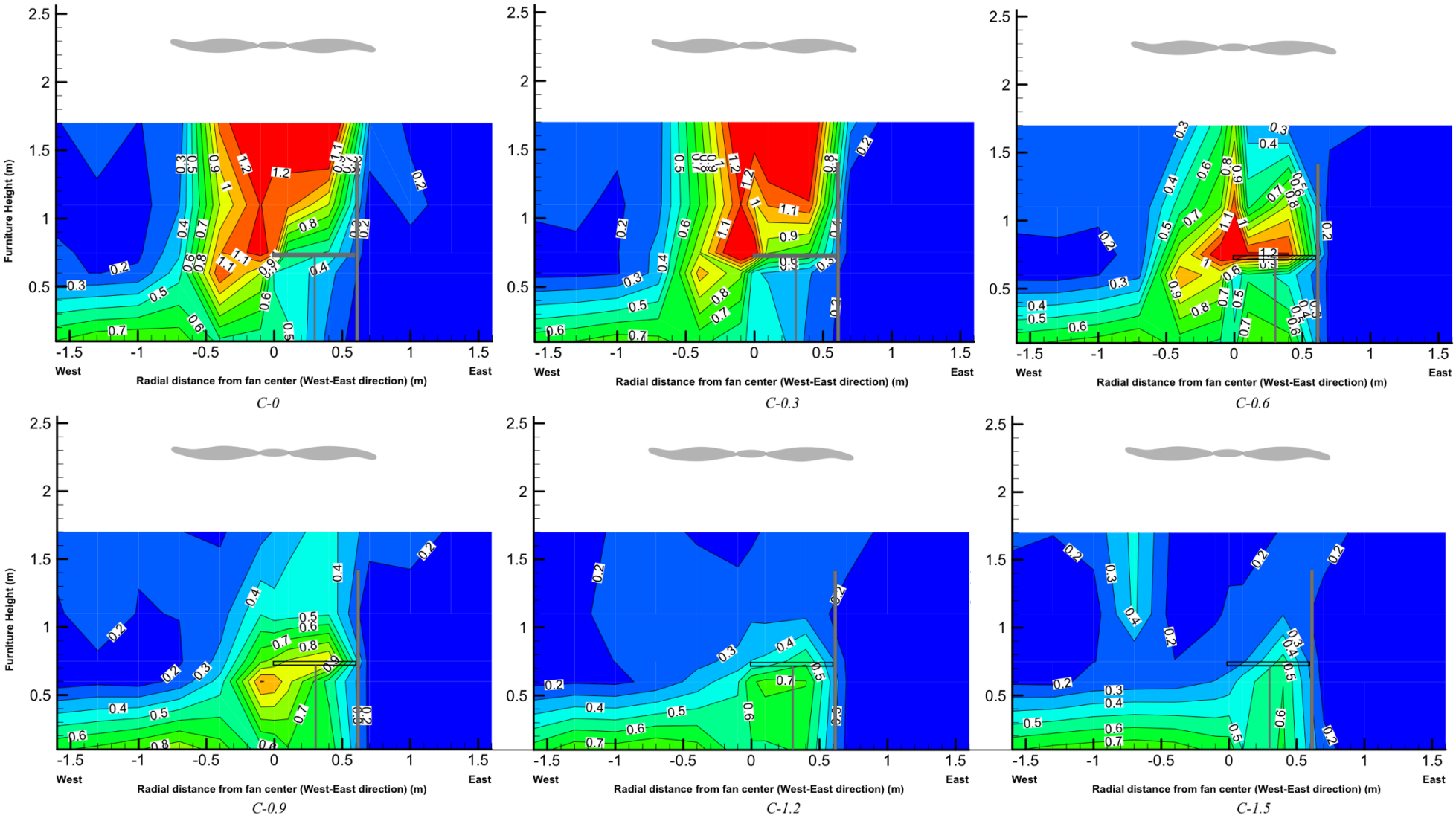

Caes 5, Vertical contours through all column positions:C-0,C-0.3,C-0.6,C-0.9,C-1.2 and C-1.5

Appendix A-6. Case 6: Fan centered above table long edge; corner partition opposite

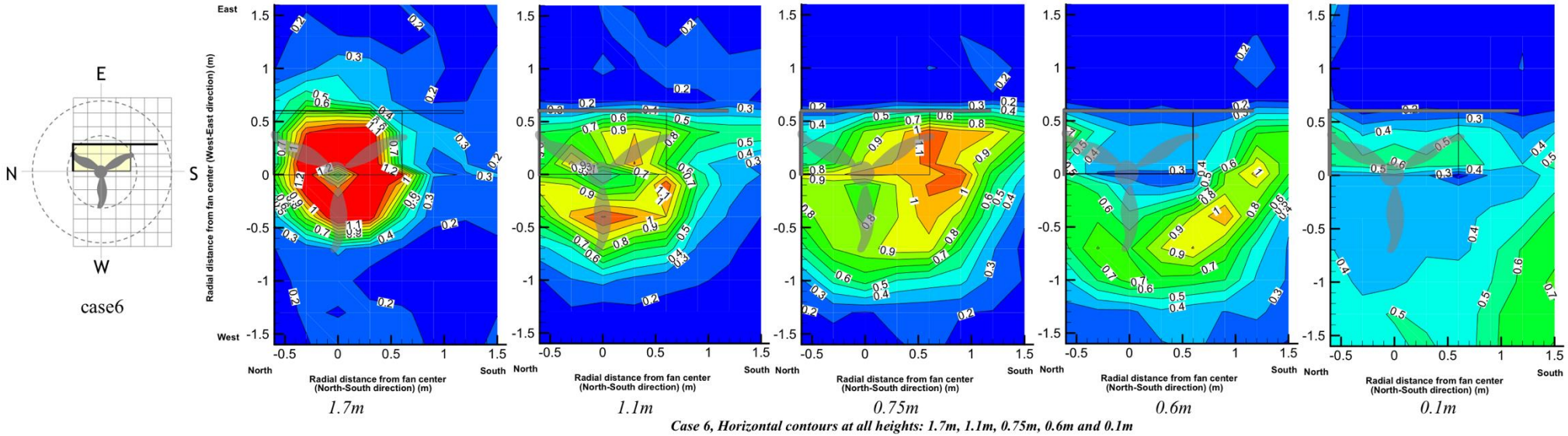

Case 6, Horizontal contours at all heights: 1.7m, 1.1m, 0.75m, 0.6m and 0.1m

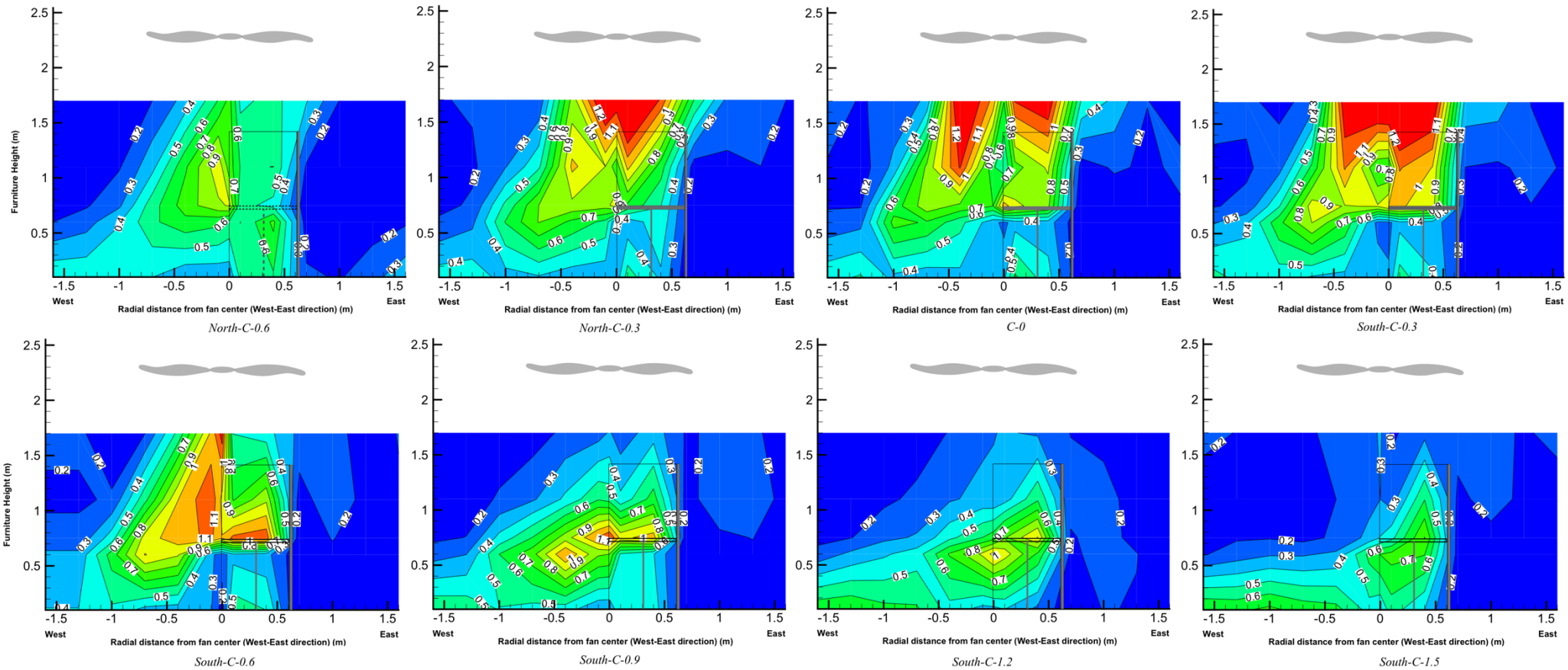

Caes 6, Vertical contours through all column positions: North-C-0.6, North-C-0.3, C-0, South-C-0.3, South-C-0.6, South-C-0.9, South-C-1.2 and South-C-1.5